動量空間 CESE 方法初探

學生: 徐煥鈞　　指導教授: 江進福

國立交通大學物理研究所碩士班

摘 要

本論文初步驗證在動量空間發展 CESE 方法的可能性, 並就線性系統、量子力學系統與非線性系統分別舉例驗證。

Conservation Element and Solution Element method in Momentum Space

student : Huan-chun, Hsu Advisors:Dr. Tsin-Fu, Jiang

Institute of Physics
National Chiao Tung University

ABSTRACT

This thesis is a preliminary study on the CESE methods in momentum space. We examined the examples of linear wave equation, a quantum mechanical problem, and a nonlinear KdV equation.

誌 謝

首先感謝我的指導老師江進福教授，從帶領渾噩的我起步，到最後補正我菜到發青的論文，期間多承您費心指導與包容。另外特別要感謝張朝亮博士無私的指教，也感謝曾給予建議協助的師長及同學們。感謝曾一同結伴前行的每一個人，不管所刻畫的記憶是深或淺、延續的影響是清或濁，我都由衷慶幸曾有你們帶我閱讀這頁頁歷程。最重要的，感謝家人無怨無盡的支持，並原諒我一次次任性妄為，這份呵護一直是我深根心底的幸福。

目 錄

List of Tables

List of Figures

符 號 說 明

u : wave function in real space

u_x : $\partial u/\partial x$

$u_{\bar{x}}$: $\Delta x\, u_x$

$\tilde{u}$: wave function in momentum space

$\tilde{u}_p$: $\partial \tilde{u}/\partial p$

$\tilde{u}_{\bar{p}}$: $\Delta p\, \tilde{u}_p$

$\mathbf{h}$: density of flux

u_e : exact solution

E : numerical error

N : number of cells of mesh

Chapter 1

Introduction

The space-time conservation element and solution element method, or the CESE method for short, originally developed by Dr. Sin-Chung Chang and then developed by Chang and co-workers, is a numerical framework with conservation law. The CESE method has many nontraditional features, such as, a unified treatment of space and time, enforced both local and global flux conservation, and so on. However, the application of CESE method in momentum space has never touched to our knowledge.

Development of the CESE method in momentum space (p-space) is motivated by a goal to avoid the troubles in boundary reflection like methods in coordinate space, and to preserve information completely for scattering states. In order to get data more completely, some numerical computations need to construct large computational domains in coordinate space, but in momentum space such a large box is not necessary. The troubles of boundary conditions can easily be overcome in momentum space. Because the value of momentum relates to the kinetic energy and physically vanishing at large value.

However, we retain the original advantages of CESE method, such as, wide application possibility, easy in implementing efficient parallel computing, compatible to complex geometries, and so on.

In this thesis, we will first briefly introduce the core ideas of CESE, and then formulate the p-space CESE method. We apply the new development to solve the simple wave equation, the convection-advection equation, a quantum mechanical problem and a nonlinear KdV equation. We found that the new method will be potentially useful in solving general time-dependent problems.

Chapter 2

Review of the CESE Method

2.1 Brief Review of the a-Scheme

In this section, we shall briefly introduce the 1D a-scheme described in Ref.[1]. Consider the PDE

$$\frac{\partial u}{\partial t} + a\,\frac{\partial u}{\partial x} = 0, \tag{2.1}$$

where the wave speed, $a \neq 0$, is a constant. Let x and t be the coordinates of a two-dimensional Euclidean space E_2. By using Gauss divergence theorem in E_2

$$\oint_{S(V)} \mathbf{h} \cdot ds = 0, \tag{2.2}$$

where $S(V)$ is the boundary of an arbitrary space-time region V in E_2, $\mathbf{h} = (a\,u, u)$ is a current density vector in E_2, and the surface element $d\mathbf{s} = d\sigma\mathbf{n}$ with $d\sigma$ and $\mathbf{n}$ being the area and the outward unit normal of a surface element on $S(V)$, respectively.

As depicted in Fig. 2.1, let E_2 be divided into non-overlapping rectangular regions and are referred as conservation elements (CEs). The CEs with the mesh point $(j, n) \in \Omega$ are denoted by $\mathrm{CE}_-(j, n)$ and $\mathrm{CE}_+(j, n)$, respectively. Each mesh point (j, n) is associated with a cross-shaped solution element.

Note that the conservation law given in Eq. (2.2) is formulated in which space and time are unified treated on equal footing. This unity of space and time is also a tenet in the following numerical development.

For any $(x, t) \in \mathrm{SE}(j, n)$, $u(x, t)$, and $\mathbf{h}(x, t)$ are approximated by $u(x, t; j, n)$ and $\mathbf{h}(x, t; j, n)$, respectively. Using the first order Taylor's expansion of $u(x, t)$ at (x_j, t^n), we define

$$u(x, t; j, n) = u_j^n + (u_x)_j^n (x - x_j) + (u_t)_j^n (t - t^n). \tag{2.3}$$

We identify u_j^n, $(u_x)_j^n$, and $(u_t)_j^n$ with the values of u, $\partial u/\partial x$, and $\partial u/\partial t$ at (x_j, t^n), respectively. Note that u_j^n, $(u_x)_j^n$, and $(u_t)_j^n$ are constants in $\mathrm{SE}(j, n)$. Requiring that

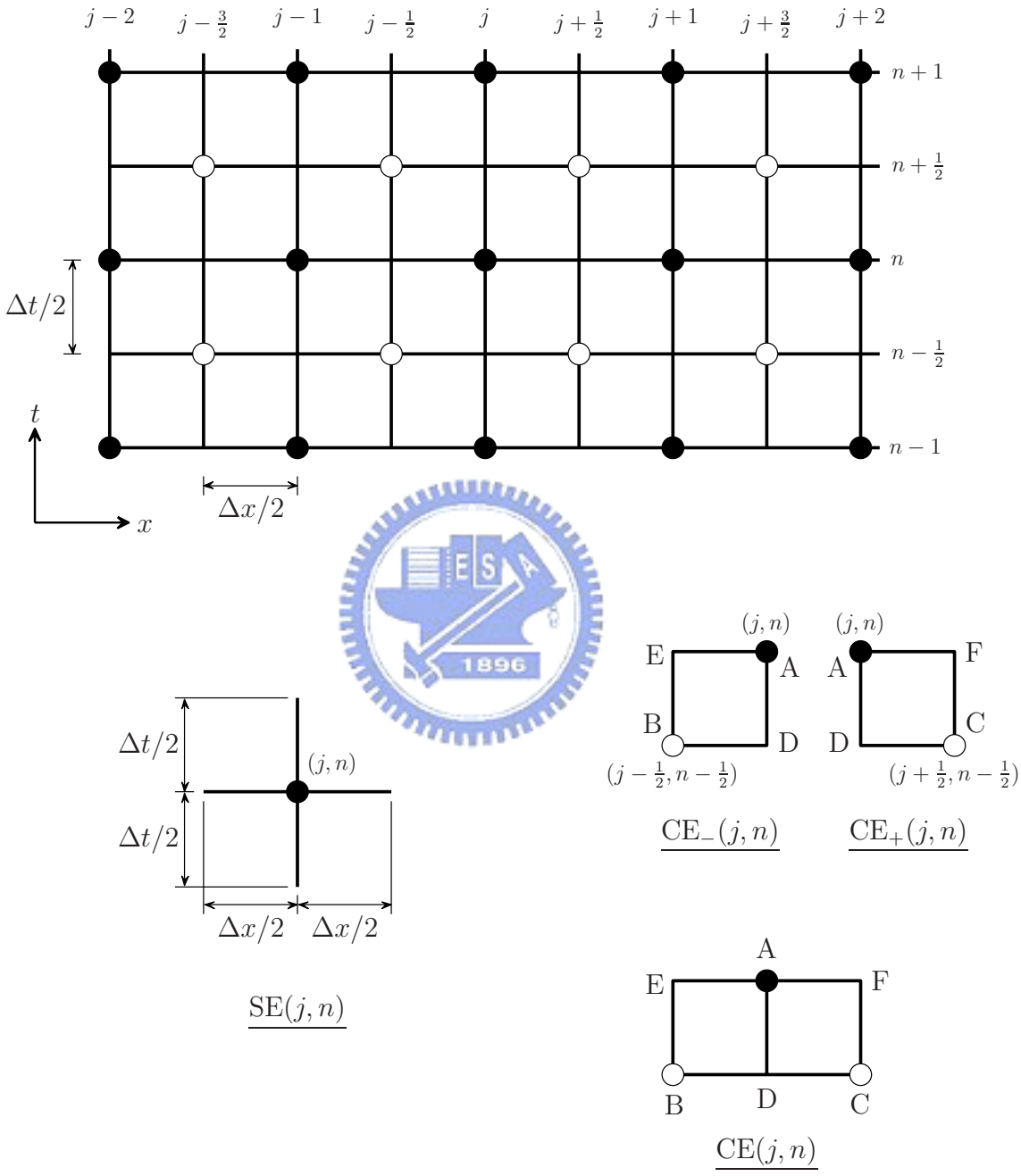

Figure 2.1. Definitions of the space-time staggered mesh, CE, and SE in E_2.

$u = u(x,t;j,n)$ satisfies Eq. (2.1) within SE(j,n), one has

$$(u_t)_j^n = -a(u_x)_j^n. \tag{2.4}$$

Substituting Eq. (2.4) into Eq. (2.3), one has

$$u(x,t;j,n) = u_j^n + [(x - x_j) - a(t - t^n)](u_x)_j^n. \tag{2.5}$$

Note that the expansion coefficients u_j^n and $(u_x)_j^n$ in Eq. (2.5) are treated as independent variables. In addition, $\mathbf{h}$ is approximated by

$$\mathbf{h}(x,t;j,n) = (a\,u(x,t;j,n), u(x,t;j,n)). \tag{2.6}$$

With the approximation, the total flux leaving the boundary of CE$_\pm(j,n)$ is

$$F_\pm(j,n) = \oint_{S(\mathrm{CE}_\pm(j,n))} \mathbf{h} \cdot .d\mathbf{s} = 0 \tag{2.7}$$

As depicted in Fig. 2.1 for CE$_-$, the outward unit normal vectors $\hat{n}$ at $\overline{\mathrm{AD}}$, $\overline{\mathrm{AE}}$, $\overline{\mathrm{BE}}$, and $\overline{\mathrm{BD}}$ are $(1,0)$, $(0,1)$, $(-1,0)$, and $(0,-1)$, respectively; and for CE$_+$, the outward unit normal vectors $\hat{n}$ at $\overline{\mathrm{AD}}$, $\overline{\mathrm{AF}}$, $\overline{\mathrm{CF}}$, and $\overline{\mathrm{CD}}$ are $(-1,0)$, $(0,1)$, $(1,0)$, and $(0,-1)$, respectively. By using Eqs. (2.5) and (2.6), it can be shown that Eq. (2.7) is equivalent to

$$(1 \mp \nu)\left[u \pm \frac{1}{4}(1 \pm \nu)u_{\bar{x}}\right]_j^n = (1 \mp \nu)\left[u \mp \frac{1}{4}(1 \pm \nu)u_{\bar{x}}\right]_{j\pm\frac{1}{2}}^{n-\frac{1}{2}}, \tag{2.8}$$

where $\nu = a\,\Delta t/\Delta x$.

Choose $1 - \nu \neq 0$ and $1 + \nu \neq 0$. Eq. (2.8) reduce to

$$\left[u \pm \frac{1}{4}(1 \pm \nu)u_{\bar{x}}\right]_j^n = \left[u \mp \frac{1}{4}(1 \pm \nu)u_{\bar{x}}\right]_{j\pm\frac{1}{2}}^{n-\frac{1}{2}}. \tag{2.9}$$

By using Eq. (2.9), u_j^n and $(u_{\bar{x}})_j^n$ can be solved in term of $u_{j\pm1/2}^{n-1/2}$ and $(u_{\bar{x}})_{j\pm1/2}^{n-1/2}$. The time-marching is then arrived by explicit iterations.

2.2 Brief Review of the a-μ-Scheme

Refer to Ref.[2], consider the dimensionless form of the one- dimensional convection-diffusion equation

$$\frac{\partial u}{\partial t} + a\frac{\partial u}{\partial x} - \mu\frac{\partial^2 u}{\partial x^2} = 0, \tag{2.10}$$

where the wave velocity a, and the viscosity coefficient μ are constants. By using Gauss divergence theorem in E_2,

$$\oint_{S(V)} \mathbf{h} \cdot d\mathbf{s} = 0,$$

where $\mathbf{h} = (a\,u - \mu\,u, u)$.

Let $u = u(x, t; j, n)$ be defined by Eq. (2.3), it satisfies Eq. (2.10). Within SE(j, n), one has

$$(u_t)_j^n = -a(u_x)_j^n. \tag{2.11}$$

Substituting Eq. (2.11) into Eq. (2.3), one has

$$u(x, t; j, n) = u_j^n + [(x - x_j) - a(t - t^n)](u_x)_j^n. \tag{2.12}$$

In addition, we have the approximation

$$\mathbf{h}(x, t; j, n) = (a\,u(x, t; j, n) - \mu\,u_x(x, t; j, n), u(x, t; j, n)). \tag{2.13}$$

The approximation defined by Eq. (2.7) of the total flux leaving the boundary of CE$_\pm(j, n)$ is

$$\begin{aligned} \frac{4}{\Delta x^2} F_\pm(j, n) = \pm\frac{1}{2}\left[(1 - \nu^2 + \xi)(u_x)_j^n + (1 - \nu^2 - \xi)(u_x)_{j\pm\frac{1}{2}}^{n-\frac{1}{2}}\right] \\ + \frac{2(1 \mp \nu)}{\Delta x}\left(u_j^n - u_{j\pm\frac{1}{2}}^{n-\frac{1}{2}}\right) = 0, \end{aligned} \tag{2.14}$$

where $\nu = a\,\Delta t/\Delta x$, $\xi = 4\mu\,\Delta t/\Delta x^2$.

By Eq. (2.14), u_j^n and $(u_x)_j^n$ can be solved in term of $u_{j\pm1/2}^{n-1/2}$ and $(u_x)_{j\pm1/2}^{n-1/2}$. The time-marching is then arrived by explicit iterations.

Chapter 3

The 1D CESE Method in Momentum Space

3.1 1D a-Scheme in Momentum Space

Eq. (2.1) can be transformed into

$$\frac{\partial \tilde{u}}{\partial t} = -i\,a\,p\,\tilde{u}, \tag{3.1}$$

by marking the Fourier transformation.

Equivalently, it can be written as

$$\nabla \cdot (0, \tilde{u}) = -i\,a\,p\,\tilde{u}, \tag{3.2}$$

where the operator $\nabla = (\partial/\partial p, \partial/\partial t)$. Consider p and t as the coordinates of a two-dimensional Euclidean space E_2. Apply the Gauss divergence theorem to E_2

$$\oint_{S(V)} \mathbf{h} \cdot d\mathbf{s} = -i\,a \int_V p\,\tilde{u}\,d\tau, \tag{3.3}$$

where $\mathbf{h} = (0, \tilde{u})$ and $(-i\,a\,p\,\tilde{u})$ is the net flux per unit volume.

Let E_2 be divided into non-overlapping rectangular regions referred to as conservation elements (CEs). The CEs with the mesh point $(j, n) \in \Omega$ are denoted by $\mathrm{CE}_-(j, n)$ and $\mathrm{CE}_+(j, n)$, respectively. Let $\mathrm{SE}(j, n)$ be the rhombus shaped area DEGF depicted in Fig. 3.1. The function value at the center of $\mathrm{CE}_\pm$ can be approximated by expanding about $u^{n-1/2}_{j\pm1/2}$ or using arithmetic mean of u^n_j and $u^{n-1/2}_{j\pm1/2}$.

For any $(p, t) \in \mathrm{SE}(j, n)$, $\tilde{u}(p, t)$ and $\mathbf{h}(p, t)$ are approximated by $\tilde{u}(p, t; j, n)$ and $\mathbf{h}(p, t; j, n)$, respectively. We define

$$\tilde{u}(p, t; j, n) = \tilde{u}^n_j + (\tilde{u}_p)^n_j (p - p_j) + (\tilde{u}_t)^n_j (t - t^n), \tag{3.4}$$

where (p_j, t^n) are the coordinates of the mesh point (j, n).

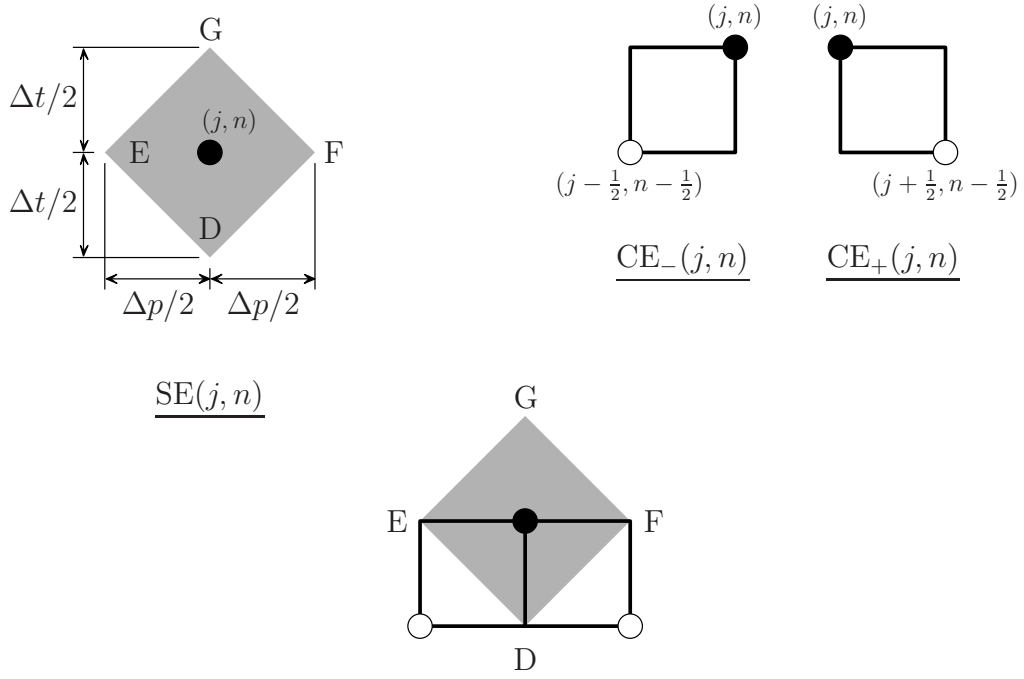

Figure 3.1. Definitions of CE and SE in E_2.

Note that $\tilde{u}_j^n$, $(\tilde{u}_p)_j^n$ and $(\tilde{u}_t)_j^n$ are constants in SE(j,n). We also have

$$\mathbf{h}(p,t;j,n) = (0, \tilde{u}(p,t;j,n)). \tag{3.5}$$

Requiring that $\tilde{u} = \tilde{u}(p,t;j,n)$ satisfies Eq. (3.1) within SE(j,n), one has

$$(\tilde{u}_t)_j^n = -i\,a\,p_j\,\tilde{u}_j^n. \tag{3.6}$$

The approximation of the total flux leaving the boundary of CE$_\pm(j,n)$ is

$$F_\pm(j,n) = \oint_{S(\mathrm{CE}_\pm(j,n))} \mathbf{h}\cdot d\mathbf{s} = -i\,a \int_{\mathrm{CE}_\pm(j,n)} p\,\tilde{u}\,d\tau. \tag{3.7}$$

By Eqs. (3.5) and (3.7), the total flux leaving CE$_\pm(j,n)$ can be derived as

$$\begin{aligned} F_\pm(j,n) &= \frac{\Delta p}{2}\left\{\tilde{u}_j^n \pm \frac{1}{4}(\tilde{u}_{\bar{p}})_j^n - \left[\tilde{u}_{j\pm\frac{1}{2}}^{n-\frac{1}{2}} \mp \frac{1}{4}(\tilde{u}_{\bar{p}})_{j\pm\frac{1}{2}}^{n-\frac{1}{2}}\right]\right\} \\ &= -i\,p_{j\pm\frac{1}{4}}\left[\tilde{u}_{j\pm\frac{1}{2}}^{n-\frac{1}{2}} \mp \frac{1}{4}(\tilde{u}_{\bar{p}})_{j\pm\frac{1}{2}}^{n-\frac{1}{2}} + \frac{\Delta t}{4}(\tilde{u}_t)_{j\pm\frac{1}{2}}^{n-\frac{1}{2}}\right]\frac{\Delta p}{2}\frac{\Delta t}{2}, \end{aligned} \tag{3.8}$$

where we use Taylor expansion to estimate the function value at the center of CE$_\pm$, in order to prepare for nonlinear situation (in Chapter 5). With the aid of Eqs. (3.6) and (3.8), $\tilde{u}_j^n$ and $(\tilde{u}_{\bar{p}})_j^n$ can be solved in terms of $\tilde{u}_{j\pm1/2}^{n-1/2}$ and $(\tilde{u}_{\bar{p}})_{j\pm1/2}^{n-1/2}$, and for further iterations,

$$\tilde{u}_{j,\ell}^n \pm \frac{1}{4}(\tilde{u}_{\bar{p}})_j^n - \left[\tilde{u}_{j\pm\frac{1}{2}}^{n-\frac{1}{2}} \mp \frac{1}{4}(\tilde{u}_{\bar{p}})_{j\pm\frac{1}{2}}^{n-\frac{1}{2}}\right] = -i\,p_{j\pm\frac{1}{4}}\frac{1}{2}\left(\tilde{u}_{j,\ell-1}^n + \tilde{u}_{j\pm\frac{1}{2}}^{n-\frac{1}{2}}\right)\frac{\Delta t}{2}. \tag{3.9}$$

We can check the convergence of $\tilde{u}_j^n$. Eq. (3.9) can also be derived from Eq. (3.7) by approximating the source term to the arithmetic mean of u_j^n and $u_{j\pm1/2}^{n-1/2}$. Here the index ℓ is the number of times that Eq. (3.9) has been iterated, and $\tilde{u}_j^n$ solved by Eq. (3.8) can be denoted by $\tilde{u}_{j,0}^n$. Using the Cauchy criterion, we define the convergence as

$$\left|\tilde{u}_{j,\ell+1}^n - \tilde{u}_{j,\ell}^n\right| < \varepsilon. \tag{3.10}$$

3.2 a-μ-Scheme in Momentum Space

In the momentum space, Eq. (2.10) can be transformed into

$$\frac{\partial \tilde{u}}{\partial t} + \left(i\,a\,p + \mu\,p^2\right)\,\tilde{u} = 0, \tag{3.11}$$

by marking the Fourier transformation. By using Gauss divergence theorem in E_2

$$\oint_{S(V)} \mathbf{h}\cdot d\mathbf{s} = -\int \left(i\,a\,p + \mu\,p^2\right)\,\tilde{u} d\tau, \tag{3.12}$$

where $\mathbf{h}$ is defined by the same as Eq. (3.5).

Requiring that $\tilde{u} = \tilde{u}(p,t;j,n)$ defined by Eq. (3.4) satisfies Eq. (3.11) within SE(j,n), one has

$$(\tilde{u}_t)_j^n = -\left(i\,a\,p_j + \mu\,p_j^2\right)\,\tilde{u}_j^n. \tag{3.13}$$

The approximation of the total flux leaving the boundary of CE$_\pm(j,n)$ is

$$F_\pm(j,n) = \oint_{S(\mathrm{CE}_\pm(j,n))} \mathbf{h}\cdot d\mathbf{s} = -\int_{\mathrm{CE}_\pm(j,n)} \left(i\,a\,p + \mu\,p^2\right)\,\tilde{u}\,d\tau. \tag{3.14}$$

By Eqs.(3.4) and (3.14), the total flux leaving CE$_+(j,n)$ can be derived as

$$\begin{aligned} F_\pm(j,n) &= \frac{\Delta p}{2}\left\{\tilde{u}_j^n \pm \frac{1}{4}(\tilde{u}_{\bar{p}})_j^n - \left[\tilde{u}_{j\pm\frac{1}{2}}^{n-\frac{1}{2}} \mp \frac{1}{4}(\tilde{u}_{\bar{p}})_{j\pm\frac{1}{2}}^{n-\frac{1}{2}}\right]\right\} \\ &= -\frac{\Delta p}{2}\frac{\Delta t}{2}\left(i\,a\,p_{j\pm\frac{1}{4}} + \mu\,p_{j\pm\frac{1}{4}}^2\right) \\ &\quad\times\left[\tilde{u}_{j\pm\frac{1}{2}}^{n-\frac{1}{2}} \mp \frac{1}{4}(\tilde{u}_{\bar{p}})_{j\pm\frac{1}{2}}^{n-\frac{1}{2}} + \frac{\Delta t}{4}(\tilde{u}_t)_{j\pm\frac{1}{2}}^{n-\frac{1}{2}}\right]. \end{aligned} \tag{3.15}$$

With the aid of Eqs. (3.15) and (3.13), $\tilde{u}_j^n$ and $(\tilde{u}_{\bar{p}})_j^n$ can be solved iteratively in terms of $\tilde{u}_{j\pm1/2}^{n-1/2}$ and $(\tilde{u}_{\bar{p}})_{j\pm1/2}^{n-1/2}$.

3.3 Numerical Results

Consider the model problem Eq. (3.1)

$$\frac{\partial \tilde{u}}{\partial t} = -i\,a\,p\,\tilde{u}, \tag{3.1}$$

and the calibrating exact solution

$$\tilde{u}_e(p,t) = \exp\left(-\frac{p^2}{2} - i\,a\,p\,t\right). \tag{3.16}$$

The initial values are given by Eq. (3.16) at $t = 0$. The numerical results of $a = 1$ at $t = 8$ are shown in Figs. 3.2 and 3.3.

Hereafter, the numerical errors will be measured by the root-mean-square form

$$E = \sqrt{\frac{1}{N-1}\sum_{s=2}^{N-1} |\tilde{u}_s^n - \tilde{u}_e(p_s, t^n)|^2}. \tag{3.17}$$

where s is the spatial index, and the p-domain is divided into N cells, and Eq. (3.17) does not consider the points of the boundaries, namely $s = 1$ and N

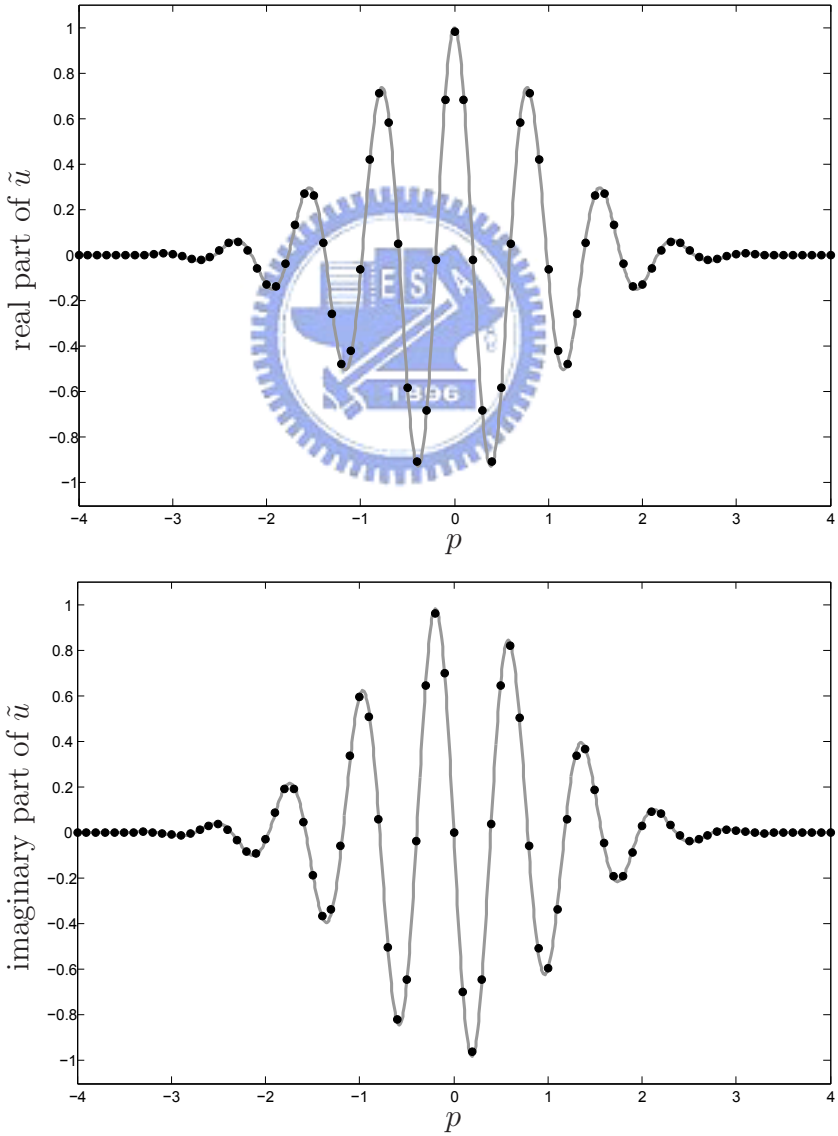

Figure 3.2. Computational results $\tilde{u}$ at $t = 8$ obtained with $p \in [-4, 4]$, $\Delta p = 0.1$, and $\Delta t = 0.08$. dot: numerical results. line: exact solution.

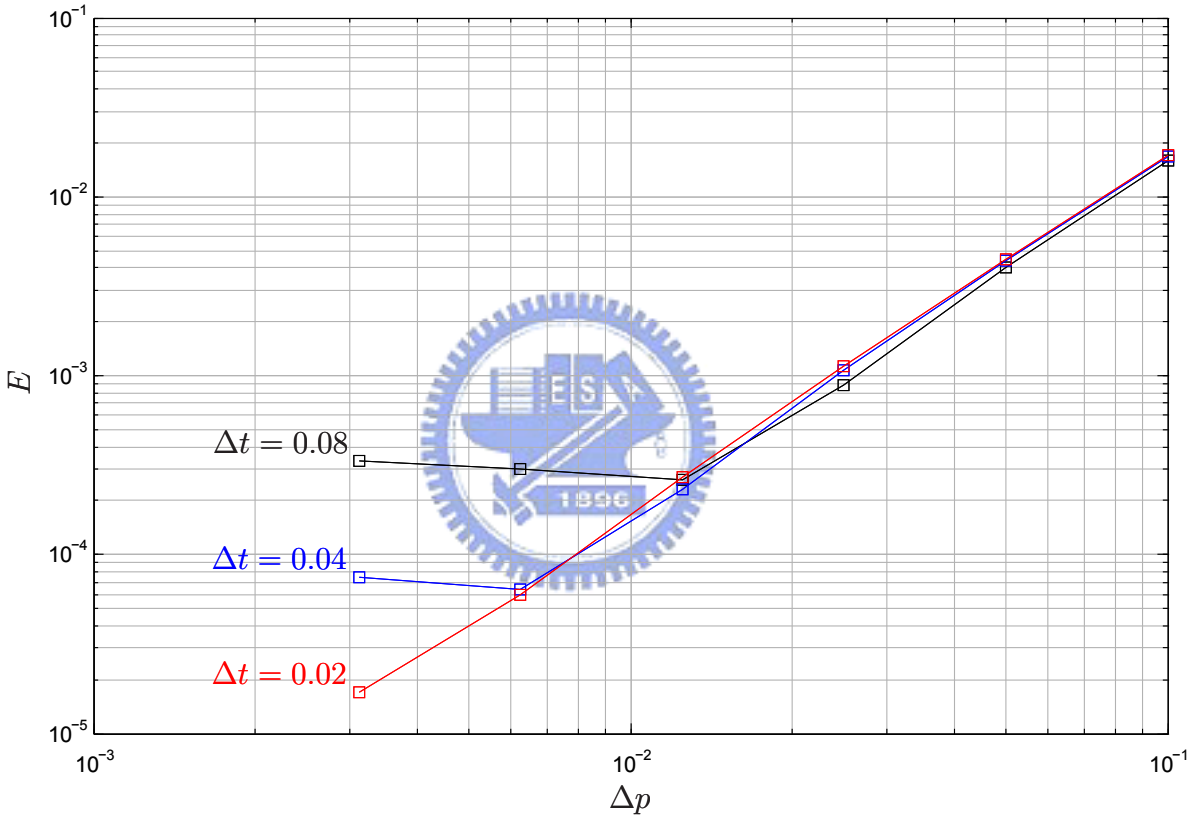

Figure 3.3. Numerical errors with $\Delta t = 0.08$, 0.04, and 0.02. ($\varepsilon = 10^{-6}$)

Before going no to the next case, we compare Fig. 3.2 with the coordinate space numerical result of Eq. (2.1) shown in Fig. 3.4. The wave in Fig. 3.4 will flow out the boundary gradually with the non-reflecting boundary condition, but Fig. 3.2 shows the momentum space wave function will not leak out at all. It is the one of advantages of momentum space method mentioned in Sec.Introduction.

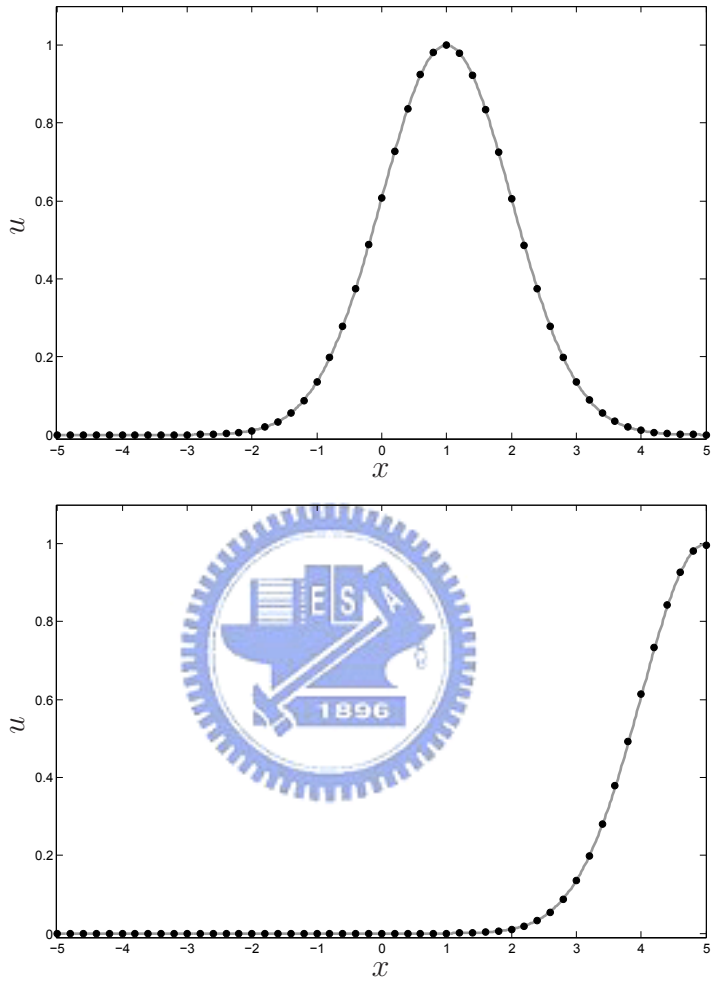

Figure 3.4. Computational results at $t = 1$ and 5 obtained with $x \in [-5, 5]$. Notice that u will flow out the boundary as time goes on.

Consider next the model problem Eq. (3.11)

$$\frac{\partial \tilde{u}}{\partial t} + \left(i\,a\,p + \mu\,p^2\right)\,\tilde{u} = 0, \tag{3.11}$$

and an exact solution

$$\tilde{u}_e(p,t) = \exp\left[-p^2 - \left(i\,a\,p + \mu\,p^2\right)\,t\right]. \tag{3.18}$$

The initial values are given by Eq. (3.18) at $t = 0$. The numerical results of $a = 1$ and $\mu = 1$ at $t = 8$ are shown in Figs. 3.5 and 3.6.

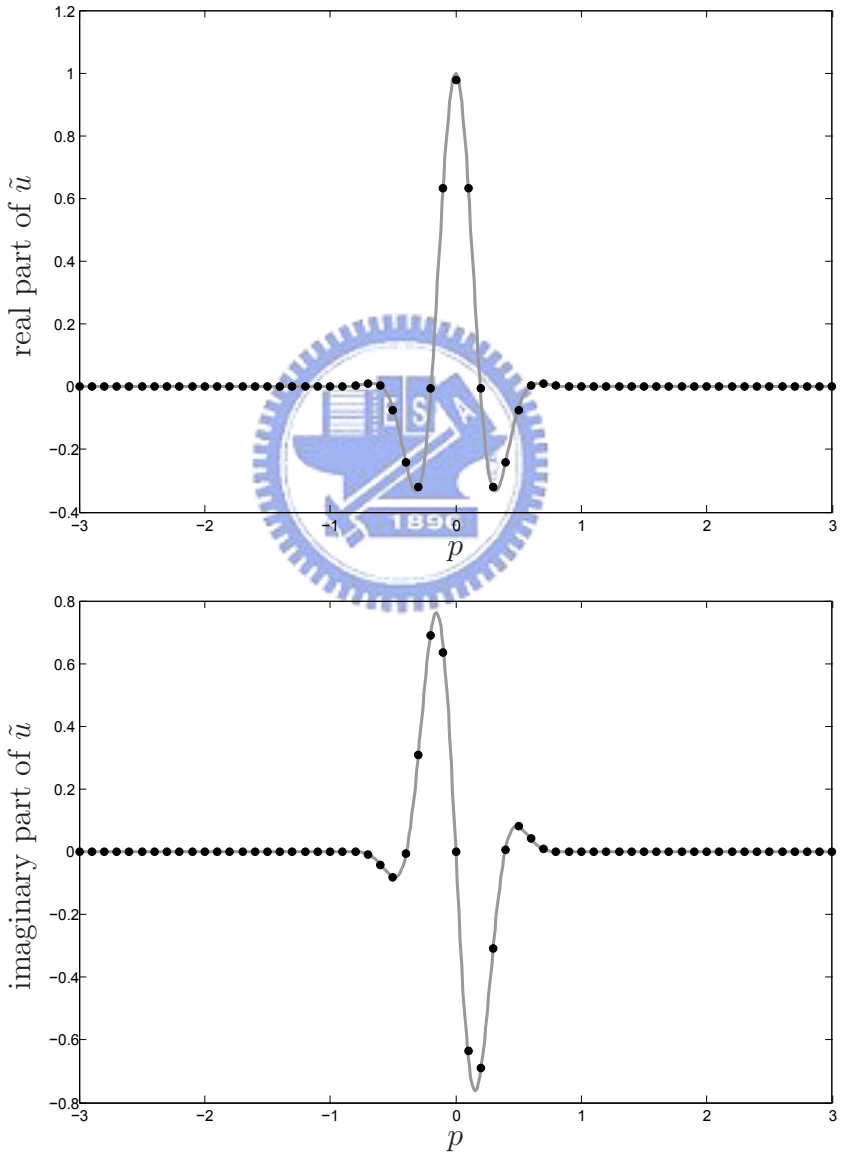

Figure 3.5. Computational results of $\tilde{u}$ at $t = 8$ obtained with $p \in [-3, 3]$ at $\Delta p = 0.1$, and $\Delta t = 0.32$.

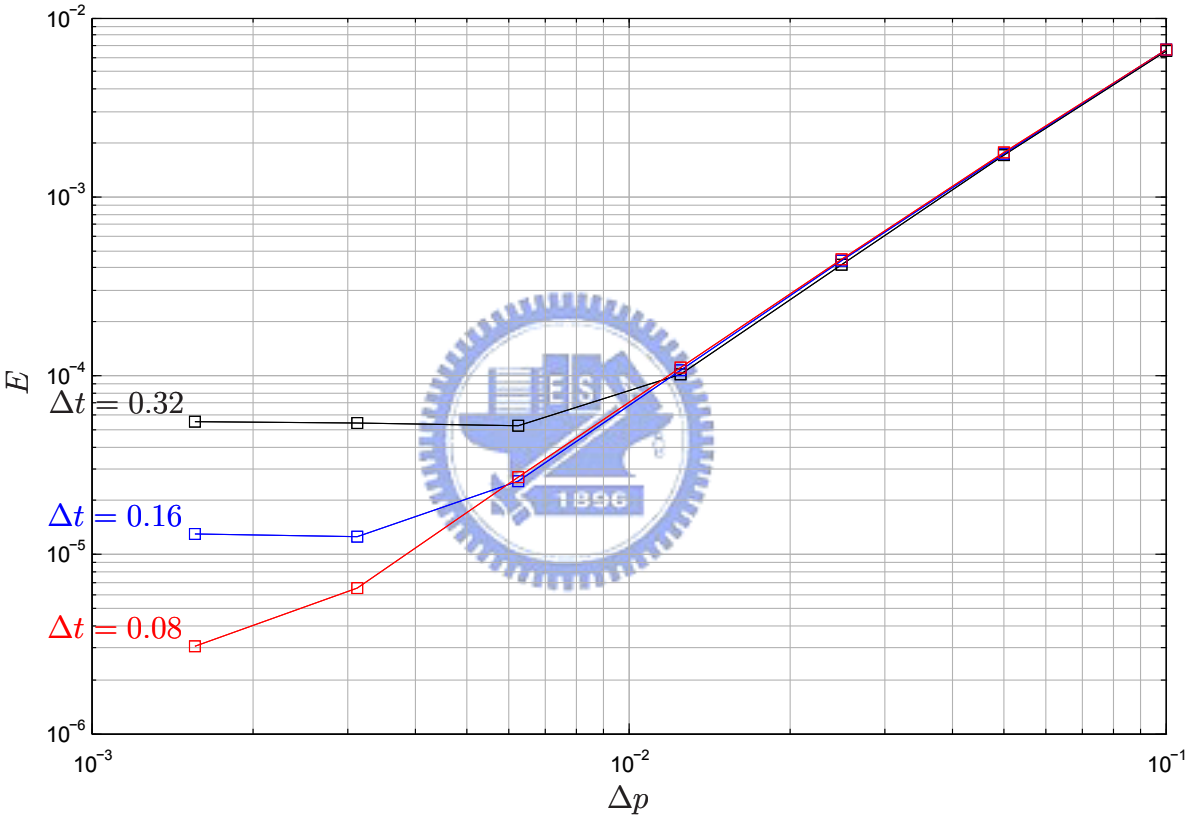

Figure 3.6. Numerical errors with $\Delta t = 0.32$, 0.16, and 0.08. ($\varepsilon = 10^{-6}$)

Chapter 4

Multidimensional Paradigm

4.1 2D a-Scheme in momentum space

Refer to [3], let's consider a regularly shaped spatial domain formed by congruent triangles (see Fig. 4.1). The center of each triangle is marked by either a hollow circle or a solid circle. As an example, point G, the center of the triangle $\triangle$BDF, is marked by a solid circle while points A, C and E, the centers of the triangles $\triangle$FMB, $\triangle$BJD and $\triangle$DLF, respectively, are marked by hollow circles. These centers are the spatial projections of the space-time mesh points used in the 2D CESE solvers.

In the 2D CESE development, assume that the mesh points are located at the time levels $n = 0, \pm 1/2, \pm 1, \pm 3/2, \ldots$ with $t = n\,\Delta t$. Furthermore, each mesh point is assigned a pair of spatial indices (j, k) according to the location of its spatial projection. Let Ω_1 denote the subset of mesh points (j, k, n) with $j, k = 0, \pm 1, \pm 2, \ldots$, and $n = 0, \pm 1, \pm 2, \ldots$. Let Ω_2 denote the subset of mesh points (j, k, n) with $j, k = 1/3, 1/3 \pm 1, 1/3 \pm 2, \ldots$, and $n = \pm 1/2, \pm 3/2, \pm 5/2, \ldots$. The set Ω is the union of the subsets Ω_1 and Ω_2.

Suppose that the points A, B, C, D, E, F, and G are at time level $t = t^n$, points A$'$, B$'$, C$'$, D$'$, E$'$, F$'$, and G$'$ are the corresponding points at $t = t^n - \Delta t/2$, and points A$''$, B$''$, C$''$, D$''$, E$''$, F$''$, and G$''$ are the corresponding points at $t = t^n + \Delta t/2$. The conservation elements associated with point G are defined to be the space-time quadrilateral cylinders GFABG$'$F$'$A$'$B$'$, GBCDG$'$B$'$C$'$D$'$, and GDEFG$'$D$'$E$'$F$'$ that are depicted in Fig. 4.2. Assume that the points O, P, Q, O$'$, P$'$, and Q$'$ are centroids of ABGFA$'$B$'$G$'$F$'$, BCDGB$'$C$'$D$'$G$'$, GDEFG$'$D$'$E$'$F$'$, ABGFA$''$B$''$G$''$F$''$, BCDGB$''$C$''$D$''$G$''$, and GDEFG$''$D$''$E$''$F$''$, respectively. The SE associated with point G is defined as the space-time icosikaitetra-hedron G$''$O$'$P$'$Q$'$ABCDEFOPQG$'$

In this section, we consider a dimensionless form of the 2D wave equation, i.e.

$$\frac{\partial u}{\partial t} + a_x \frac{\partial u}{\partial x} + a_y \frac{\partial u}{\partial y} = 0. \tag{4.1}$$

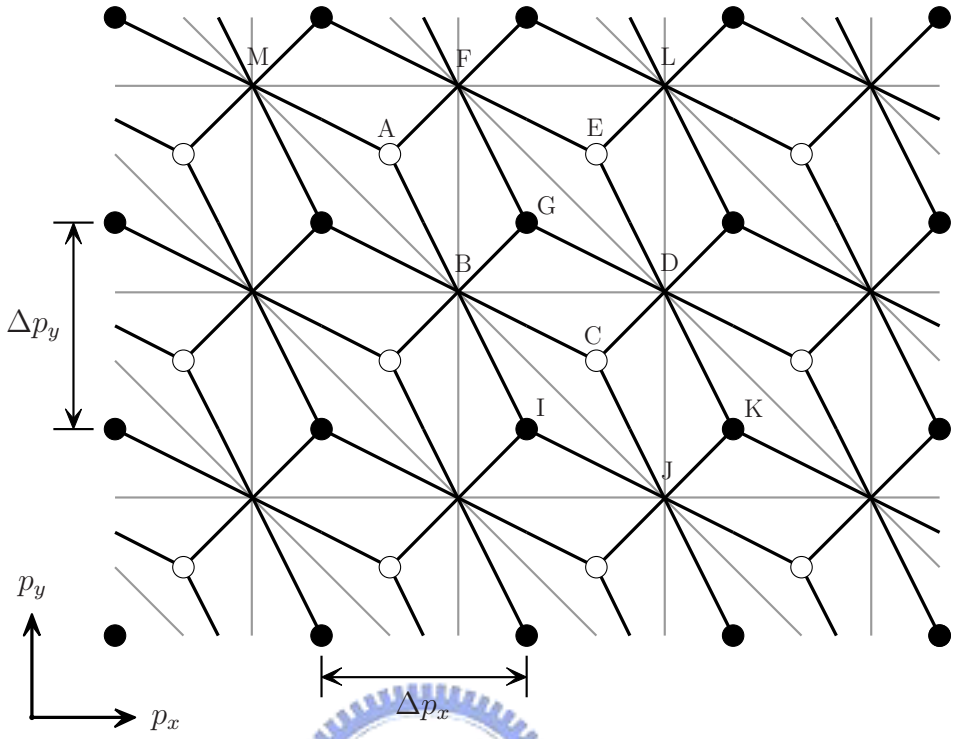

Figure 4.1. Spatial mesh in E_3. The spatial projections of the mesh points $(j, k, n) \in \Omega_1$ are marked by solid circles; the others marked by hollow circles belong to Ω_2.

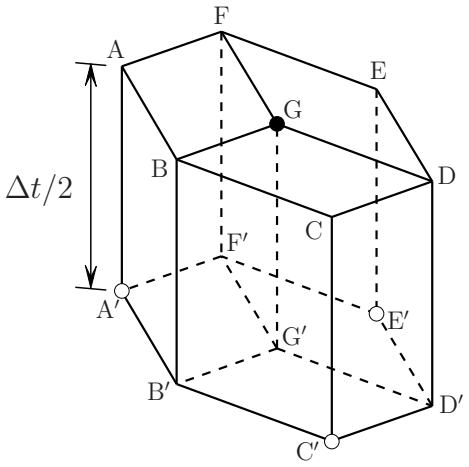

Figure 4.2. Definitions of CE in E_3.

By marking Fourier transformation, Eq. (4.1) can be transformed into

$$\frac{\partial \tilde{u}}{\partial t} = -i\,(a_x\,p_x + a_y\,p_y). \tag{4.2}$$

Let p_x, p_y and t be considered as the coordinates of a 3D Euclidean space E_3 and j and k be spatial mesh indices. By repeating the above-mentioned method and using the first order Taylor's expansion of $\tilde{u}(p_x, p_y, t)$,

$$\begin{aligned}\tilde{u}(p_x, p_y, t; j, k, n) = \tilde{u}^n_{j,k} + (\tilde{u}_{p_x})^n_{j,k}\,(p_x - p_{xj}) + (\tilde{u}_{p_y})^n_{j,k}\,(p_y - p_{yk}) \\ + (\tilde{u}_t)^n_{j,k}\,(t - t^n).\end{aligned} \tag{4.3}$$

at (p_{xj}, p_{yk}, t^n), one can solved $\tilde{u}^n_{j,k}$, $(\tilde{u}_{p_x})^n_{j,k}$ and $(\tilde{u}_{p_y})^n_{j,k}$

The marching variables at any $(j, k, n) \in \Omega_1$ are determined in terms of those associated with the mesh points $(j - 2/3, k + 1/3, n - 1/2)$, $(j + 1/3, k - 2/3, n - 1/2)$, and $(j + 1/3, k + 1/3, n - 1/2)$. The three CEs, as the quadrilaterals ABGF, CDGB, and EFGD depicted in Fig. 4.2, associated with the mesh points mentioned above are denoted by CE_r, $r = 1, 2, 3$, respectively. The approximations of the total flux leaving the boundaries of these CEs are

$$\begin{aligned}F_{\mathrm{CE}_1}(j,k,n) &= \Delta V \left\{ \left[\tilde{u} - \frac{1}{3}\tilde{u}_{\bar{p}_x} + \frac{1}{6}\tilde{u}_{\bar{p}_y} \right]^n_{j,k} - \left[\tilde{u} + \frac{1}{3}\tilde{u}_{\bar{p}_x} - \frac{1}{6}\tilde{u}_{\bar{p}_y} \right]^{n-\frac{1}{2}}_{j-\frac{2}{3},k+\frac{1}{3}} \right\} \\ &= -i\,\Delta V \frac{\Delta t}{2} \left[a_x\,p_{x,j-\frac{1}{3}} + a_y\,p_{y,k+\frac{1}{6}} \right] \\ &\quad \times \left[\tilde{u} + \frac{1}{3}\tilde{u}_{\bar{p}_x} - \frac{1}{6}\tilde{u}_{\bar{p}_z} + \frac{\Delta t}{4}\tilde{u}_t \right]^{n-\frac{1}{2}}_{j-\frac{2}{3},k+\frac{1}{3},},\end{aligned} \tag{4.4}$$

$$\begin{aligned}F_{\mathrm{CE}_2}(j,k,n) &= \Delta V \left\{ \left[\tilde{u} + \frac{1}{6}\tilde{u}_{\bar{p}_x} - \frac{1}{3}\tilde{u}_{\bar{p}_y} \right]^n_{j,k} - \left[\tilde{u} - \frac{1}{6}\tilde{u}_{\bar{p}_x} + \frac{1}{3}\tilde{u}_{\bar{p}_y} \right]^{n-\frac{1}{2}}_{j+\frac{1}{3},k-\frac{2}{3}} \right\} \\ &= -i\,\Delta V \frac{\Delta t}{2} \left[a_x\,p_{x,j+\frac{1}{6}} + a_y\,p_{y,k-\frac{1}{3}} \right] \\ &\quad \times \left[\tilde{u} - \frac{1}{6}\tilde{u}_{\bar{p}_x} + \frac{1}{3}\tilde{u}_{\bar{p}_z} + \frac{\Delta t}{4}\tilde{u}_t \right]^{n-\frac{1}{2}}_{j+\frac{1}{3},k-\frac{2}{3},},\end{aligned} \tag{4.5}$$

and

$$\begin{aligned}F_{\mathrm{CE}_3}(j,k,n) &= \Delta V \left\{ \left[\tilde{u} + \frac{1}{6}\tilde{u}_{\bar{p}_x} + \frac{1}{6}\tilde{u}_{\bar{p}_y} \right]^n_{j,k} - \left[\tilde{u} - \frac{1}{6}\tilde{u}_{\bar{p}_x} - \frac{1}{6}\tilde{u}_{\bar{p}_y} \right]^{n-\frac{1}{2}}_{j+\frac{1}{3},k+\frac{1}{3}} \right\} \\ &= -i\,\Delta V \frac{\Delta t}{2} \left[a_x\,p_{x,j+\frac{1}{6}} + a_y\,p_{y,k+\frac{1}{6}} \right] \\ &\quad \times \left[\tilde{u} - \frac{1}{6}\tilde{u}_{\bar{p}_x} - \frac{1}{6}\tilde{u}_{\bar{p}_z} + \frac{\Delta t}{4}(\tilde{u}_t) \right]^{n-\frac{1}{2}}_{j+\frac{1}{3},k+\frac{1}{3},}.\end{aligned} \tag{4.6}$$

Similarly, The marching variables at any $(j, k, n) \in \Omega_2$ are determined in terms of those associated with the mesh points $(j - 1/3, k + 2/3, n - 1/2)$, $(j - 1/3, k - 1/3, n - 1/2)$, and

$(j+2/3, k-1/3, n-1/2)$. The approximations of the total flux leaving the boundaries of these CEs, as the quadrilaterals IJCB, KDCJ, and GBCD depicted in Fig. 4.2, are

$$\begin{aligned} F_{\mathrm{CE}_1}(j,k,n) &= \Delta V \left\{ \left[\tilde{u} - \frac{1}{6}\tilde{u}_{\bar{p}_x} + \frac{1}{3}\tilde{u}_{\bar{p}_y} \right]_{j,k}^{n} - \left[\tilde{u} + \frac{1}{6}\tilde{u}_{\bar{p}_x} - \frac{1}{3}\tilde{u}_{\bar{p}_y} \right]_{j-\frac{1}{3},k+\frac{2}{3}}^{n-\frac{1}{2}} \right\} \\ &= -i\,\Delta V \frac{\Delta t}{2} \left[a_x\, p_{x,j-\frac{1}{6}} + a_y\, p_{y,k+\frac{1}{3}} \right] \\ &\quad \times \left[\tilde{u} + \frac{1}{6}\tilde{u}_{\bar{p}_x} - \frac{1}{3}\tilde{u}_{\bar{p}_z} + \frac{\Delta t}{4}\tilde{u}_t \right]_{j-\frac{1}{3},k+\frac{2}{3},}^{n-\frac{1}{2}}, \end{aligned} \tag{4.7}$$

$$\begin{aligned} F_{\mathrm{CE}_2}(j,k,n) &= \Delta V \left\{ \left[\tilde{u} - \frac{1}{6}\tilde{u}_{\bar{p}_x} - \frac{1}{6}\tilde{u}_{\bar{p}_y} \right]_{j,k}^{n} - \left[\tilde{u} + \frac{1}{6}\tilde{u}_{\bar{p}_x} + \frac{1}{6}\tilde{u}_{\bar{p}_y} \right]_{j-\frac{1}{3},k-\frac{1}{3}}^{n-\frac{1}{2}} \right\} \\ &= -i\,\Delta V \frac{\Delta t}{2} \left[a_x\, p_{x,j-\frac{1}{6}} + a_y\, p_{y,k-\frac{1}{6}} \right] \\ &\quad \times \left[\tilde{u} + \frac{1}{6}\tilde{u}_{\bar{p}_x} + \frac{1}{6}\tilde{u}_{\bar{p}_z} + \frac{\Delta t}{4}\tilde{u}_t \right]_{j-\frac{1}{3},k-\frac{1}{3},}^{n-\frac{1}{2}}, \end{aligned} \tag{4.8}$$

and

$$\begin{aligned} F_{\mathrm{CE}_3}(j,k,n) &= \Delta V \left\{ \left[\tilde{u} + \frac{1}{3}\tilde{u}_{\bar{p}_x} - \frac{1}{6}\tilde{u}_{\bar{p}_y} \right]_{j,k}^{n} - \left[\tilde{u} - \frac{1}{3}\tilde{u}_{\bar{p}_x} + \frac{1}{6}\tilde{u}_{\bar{p}_y} \right]_{j+\frac{2}{3},k-\frac{1}{3}}^{n-\frac{1}{2}} \right\} \\ &= -i\,\Delta V \frac{\Delta t}{2} \left[a_x\, p_{x,j+\frac{1}{3}} + a_y\, p_{y,k-\frac{1}{6}} \right] \\ &\quad \times \left[\tilde{u} - \frac{1}{3}\tilde{u}_{\bar{p}_x} + \frac{1}{6}\tilde{u}_{\bar{p}_z} + \frac{\Delta t}{4}(\tilde{u}_t) \right]_{j+\frac{2}{3},k-\frac{1}{3},}^{n-\frac{1}{2}}. \end{aligned} \tag{4.9}$$

4.2 3D a-Scheme in momentum space

Refer to [4] and [5], let's consider the tetrahedron ABCD in Fig. 4.3. Points G and H are the centroids of ABCD and ABCP, respectively. The two tetrahedrons share the face ABC. Suppose that the points G, H, A, B, C and D are at time level $t = t^n$, points G′, H′, A′, B′, C′ and D′ are the corresponding points at $t = t^n - \Delta t/2$, and points G″, H″, A″, B″, C″ and D″ are the corresponding points at $t = t^n + \Delta t/2$. The cylinder GABCHG′A′B′C′H′ is defined as one CE associated with the space-time mesh point G, with GABCH as its spatial base.

In a similar fashion, three additional CEs associated with the mesh point $\mathrm{G}(j,n)$ can be constructed by considering in turn the three tetrahedrons that share with ABCD one of its other three surfaces. Assume points E, F and I are the centroids of the other three neighboring tetrahedrons sharing BCD, ABD and CDA, respectively. The points E′, F′ and I′ are the corresponding points at time level $t = t^n - \Delta t/2$. Then the other three CEs are defined as the cylinder GBCDEG′B′C′D′E′, GABDFG′A′B′D′F′ and GCDAIG′C′D′A′I′,

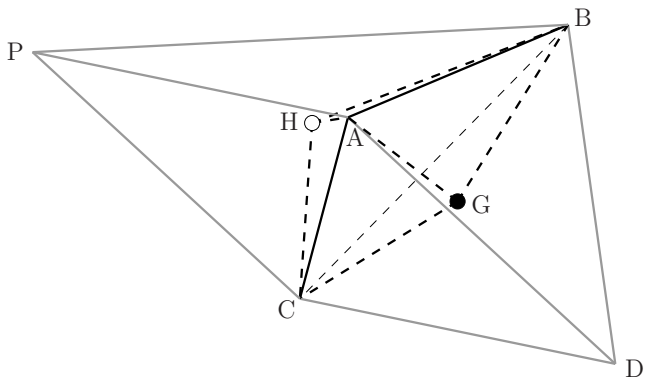

Figure 4.3. Definitions of 3D CE. G and H are the centroids of tetrahedrons ABCD and ABCP, respectively. They are the spatial projections of mesh points at a whole-integer and half-integer time level, respectively. The triangular bipyramid GABCH is one of the spatial projections of CEs associated with mesh point G.

respectively, i.e., the polyhedrons GBCDE, GABDF and GCDAI are the spatial projections of the other three CEs associated with mesh point $\mathrm{G}(j,n)$.

Similar to that in one and two spatial dimensions, there is only one solution element (SE) associated with each mesh point. Here the SE associated with point G is defined as the union of G′A′B′G″A″B″, G′B′C′G″B″C″, G′A′C′G″A″C″, G′D′C′G″D″C″, G′D′B′G″D″B″, G′A′D′G″A″D″, AHBECFDI and their immediate neighborhoods.

In this section, we consider a dimensionless form of the 3D wave equation, i.e.

$$\frac{\partial u}{\partial t} + a_x \frac{\partial u}{\partial x} + a_y \frac{\partial u}{\partial y} + a_z \frac{\partial u}{\partial z} = 0. \tag{4.10}$$

By marking Fourier transformation, Eq. (4.10) can be transformed into

$$\frac{\partial \tilde{u}}{\partial t} = -i(a_x p_x + a_y p_y + a_z p_z). \tag{4.11}$$

Let p_x, p_y, p_z and t be considered as the coordinates of a 4D Euclidean space E_4. Furthermore, each mesh point is assigned a set of spatial indices (j,k,h) according to the location of its spatial projection. By using the first order Taylor's expansion of $\tilde{u}(p_x,p_y,p_z,t)$

$$\begin{aligned}\tilde{u}(p_x,p_y,p_z,t) = \tilde{u}^n_{j,k,h} + (\tilde{u}_{p_x})^n_{j,k,h}(p_x - p_{x,j}) + (\tilde{u}_{p_y})^n_{j,k,h}(p_y - p_{y,k}) \\ + (\tilde{u}_{p_z})^n_{j,k,h}(p_z - p_{z,h}) + (\tilde{u}_t)^n_{j,k,h}(t - t^n),\end{aligned} \tag{4.12}$$

at $(p_{xj}, p_{yk}, p_{zh}, t^n)$, one can solved $\tilde{u}^n_{j,k,h}$, $(\tilde{u}_{p_x})^n_{j,k,h}$, $(\tilde{u}_{p_y})^n_{j,k,h}$, $(\tilde{u}_{p_z})^n_{j,k,h}$.

In this section, we construct a regularly shaped spatial mesh formed by the tetrahedrons defined by Fig. 4.4, and let the vector $(\Delta p_x, \Delta p_y, \Delta p_z)$ be denoted by the indices $(1,1,1)$. In a unit of building blocks including six forms depicted in Fig. 4.5 – 4.10, assuming that a reference point is denoted by (j_d,k_d,h_d), we assign the spatial projections

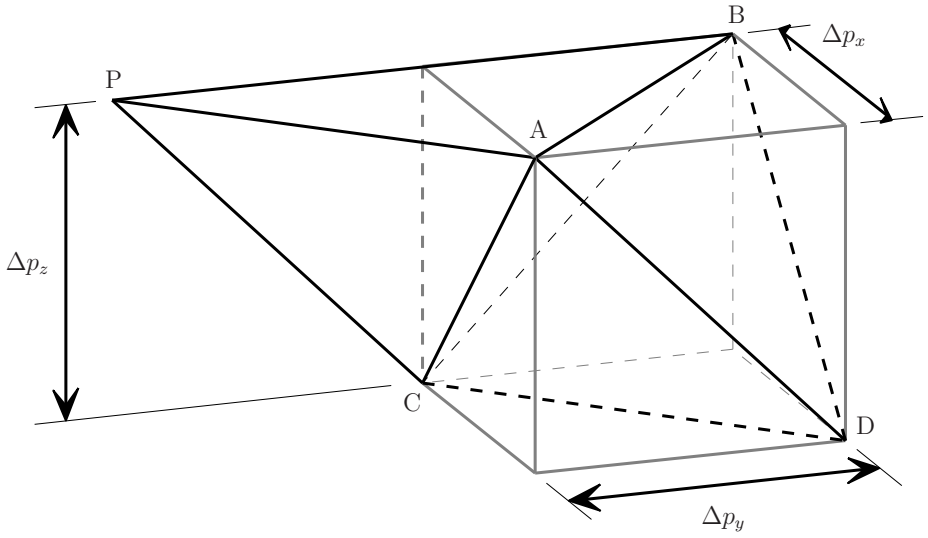

Figure 4.4. The tetrahedron ABCD is embedded inside the cube (gray line). Each vertex of ABCD is a vertex of the cube, and each edge is a diagonal of one of the cube's faces. One of four other tetrahedrons inside the cube combines with its neighboring one in another cube to the tetrahedron ABCP.

of the twelve mesh points at time level n_d to $(j_d - \frac{3}{4}, k_d, h_d - \frac{3}{4})$, $(j_d - \frac{1}{4}, k_d, h_d - \frac{1}{4})$, $(j_d - \frac{3}{4}, k_d - 1, h_d - \frac{1}{4})$, $(j_d - \frac{1}{4}, k_d - 1, h_d - \frac{3}{4})$, $(j_d + \frac{1}{2}, k_d - \frac{1}{2}, h_d - \frac{1}{2})$, $(j_d + \frac{1}{2}, k_d + \frac{1}{2}, h_d - \frac{1}{2})$, $(j_d + \frac{1}{4}, k_d, h_d + \frac{1}{4})$, $(j_d + \frac{3}{4}, k_d, h_d + \frac{3}{4})$, $(j_d + \frac{1}{4}, k_d - 1, h_d + \frac{3}{4})$, $(j_d + \frac{3}{4}, k_d - 1, h_d + \frac{1}{4})$, $(j_d - \frac{1}{2}, k_d - \frac{1}{2}, h_d + \frac{1}{2})$, and $(j_d - \frac{1}{2}, k_d + \frac{1}{2}, h_d + \frac{1}{2})$, and assign the spatial projections of the other mesh points at time index $n_d - \frac{1}{2}$ to $(j_d + \frac{1}{4}, k_d + 1, h_d - \frac{3}{4})$, $(j_d + \frac{3}{4}, k_d + 1, h_d - \frac{1}{4})$, $(j_d + \frac{1}{4}, k_d, h_d - \frac{1}{4})$, $(j_d + \frac{3}{4}, k_d, h_d - \frac{3}{4})$, $(j_d - \frac{1}{2}, k_d + \frac{1}{2}, h_d - \frac{1}{2})$, $(j_d - \frac{1}{2}, k_d - \frac{1}{2}, h_d - \frac{1}{2})$, $(j_d - \frac{3}{4}, k_d + 1, h_d + \frac{1}{4})$, $(j_d - \frac{1}{4}, k_d + 1, h_d + \frac{3}{4})$, $(j_d - \frac{3}{4}, k_d, h_d + \frac{3}{4})$, $(j_d - \frac{1}{4}, k_d, h_d + \frac{1}{4})$, $(j_d + \frac{1}{2}, k_d + \frac{1}{2}, h_d + \frac{1}{2})$, and $(j_d + \frac{1}{2}, k_d - \frac{1}{2}, h_d + \frac{1}{2})$, respectively. The units of building blocks can fill whole space with $j_b, k_b, h_b = 0, \pm 2, \pm 4, \ldots$.

(a) The CEs according to the mesh point $(j_d - \frac{3}{4}, k_d, h_d - \frac{3}{4}, n_d)$, or $(j_d + \frac{1}{4}, k_d, h_d + \frac{1}{4}, n_d)$, or $(j_d + \frac{1}{4}, k_d + 1, h_d - \frac{3}{4}, n_d - \frac{1}{2})$, or $(j_d - \frac{3}{4}, k_d + 1, h_d + \frac{1}{4}, n_d - \frac{1}{2})$, denoted by $\mathrm{G}(j, k, h)$ are shown in Fig. 4.5. Hereafter points E, F, G, H, and I are the centroids of tetrahedrons BCDR, ABDO, ABCD, ABCP and ACDQ, respectively. Consider the spatial projections of CEs GBCDE, GABDF, GABCH and GACDI in Fig. 4.5, in which the spatial projections of mesh points E, F, H, I can be denoted by $(j - \frac{1}{2}, k, h)$, $(j, k, h - \frac{1}{2})$, $(j + \frac{1}{4}, k + \frac{1}{2}, h + \frac{1}{4})$, $(j + \frac{1}{4}, k - \frac{1}{2}, h + \frac{1}{4})$, respectively, and the spatial centroids of these CEs are denoted by $(j - \frac{1}{4}, k, h + \frac{1}{20})$, $(j + \frac{1}{20}, k, h - \frac{1}{4})$, $(j + \frac{1}{10}, k + \frac{3}{10}, h + \frac{1}{10})$, $(j + \frac{1}{10}, k - \frac{3}{10}, h + \frac{1}{10})$, respectively.

Thus the approximations of the total flux leaving the boundaries of CEs GBCDE (denoted by CE_1), GABDF (denoted by CE_2), GABCH (denoted by CE_3) and GACDI

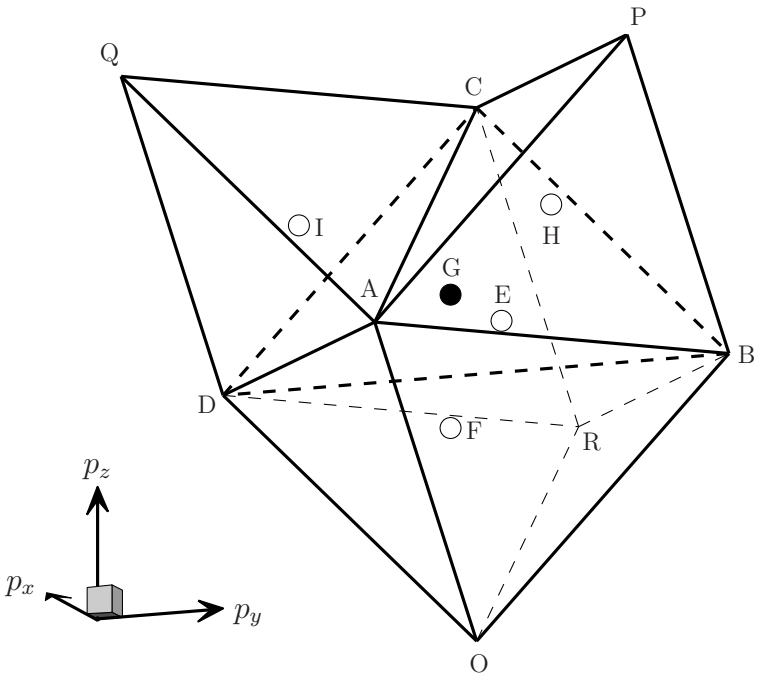

Figure 4.5. Spatial building block (a) in E_4.

(denoted by CE_4) in Fig. 4.5 are

$$\begin{aligned} F_{\mathrm{CE}_1}(j,k,h,n) &= \Delta V \left\{ \left[\tilde{u} - \frac{1}{4}\tilde{u}_{\bar{p}_x} + \frac{1}{20}\tilde{u}_{\bar{p}_z} \right]^{n}_{j,k,h} - \left[\tilde{u} + \frac{1}{4}\tilde{u}_{\bar{p}_x} + \frac{1}{20}\tilde{u}_{\bar{p}_z} \right]^{n-\frac{1}{2}}_{j-\frac{1}{2},k,h} \right\} \\ &= -i \left(a_x\, p_{x,j-\frac{1}{4}} + a_y\, p_{y,k} + a_z\, p_{z,h+\frac{1}{20}} \right) \\ &\quad \times \left[\tilde{u} + \frac{1}{4}\tilde{u}_{\bar{p}_x} + \frac{1}{20}\tilde{u}_{\bar{p}_z} + \frac{\Delta t}{4}\tilde{u}_t \right]^{n-\frac{1}{2}}_{j-\frac{1}{2},k,h} \Delta V \frac{\Delta t}{2}, \end{aligned} \tag{4.13}$$

$$\begin{aligned} F_{\mathrm{CE}_2}(j,k,h,n) &= \Delta V \left\{ \left[\tilde{u} + \frac{1}{20}\tilde{u}_{\bar{p}_x} - \frac{1}{4}\tilde{u}_{\bar{p}_z} \right]^{n}_{j,k,h} - \left[\tilde{u} + \frac{1}{20}\tilde{u}_{\bar{p}_x} + \frac{1}{4}\tilde{u}_{\bar{p}_z} \right]^{n-\frac{1}{2}}_{j,k,h-1/2} \right\} \\ &= -i \left(a_x\, p_{x,j+\frac{1}{20}} + a_y\, p_{y,k} + a_z\, p_{z,h-\frac{1}{4}} \right) \\ &\quad \times \left[\tilde{u} + \frac{1}{20}\tilde{u}_{\bar{p}_x} + \frac{1}{4}\tilde{u}_{\bar{p}_z} + \frac{\Delta t}{4}\tilde{u}_t \right]^{n-\frac{1}{2}}_{j,k,h-\frac{1}{2}} \Delta V \frac{\Delta t}{2}, \end{aligned} \tag{4.14}$$

$$\begin{aligned} F_{\mathrm{CE}_3}(j,k,h,n) &= \Delta V \Bigg\{ \left[\tilde{u} + \frac{1}{10}\tilde{u}_{\bar{p}_x} + \frac{3}{10}\tilde{u}_{\bar{p}_y} + \frac{1}{10}\tilde{u}_{\bar{p}_z} \right]^{n}_{j,k,h} \\ &\quad - \left[\tilde{u} - \frac{3}{20}\tilde{u}_{\bar{p}_x} - \frac{1}{5}\tilde{u}_{\bar{p}_y} - \frac{3}{20}\tilde{u}_{\bar{p}_z} \right]^{n-\frac{1}{2}}_{j+\frac{1}{4},k+\frac{1}{2},h+\frac{1}{4}} \Bigg\} \\ &= -i \left(a_x\, p_{x,j+\frac{1}{10}} + a_y\, p_{y,k+\frac{3}{10}} + a_z\, p_{z,h+\frac{1}{10}} \right) \\ &\quad \times \left[\tilde{u} - \frac{3}{20}\tilde{u}_{\bar{p}_x} - \frac{1}{5}\tilde{u}_{\bar{p}_y} - \frac{3}{20}\tilde{u}_{\bar{p}_z} + \frac{\Delta t}{4}\tilde{u}_t \right]^{n-\frac{1}{2}}_{j+\frac{1}{4},k+\frac{1}{2},h+\frac{1}{4}} \Delta V \frac{\Delta t}{2} \end{aligned} \tag{4.15}$$

and

$$
\begin{aligned}
F_{\mathrm{CE}_4}(j,k,h,n) = \Delta V \Bigg\{ & \left[\tilde{u} + \frac{1}{10}\tilde{u}_{\bar{p}_x} - \frac{3}{10}\tilde{u}_{\bar{p}_y} + \frac{1}{10}\tilde{u}_{\bar{p}_z} \right]_{j,k,h}^{n} \\
& - \left[\tilde{u} - \frac{3}{20}\tilde{u}_{\bar{p}_x} + \frac{1}{5}\tilde{u}_{\bar{p}_y} - \frac{3}{20}\tilde{u}_{\bar{p}_z} \right]_{j+\frac{1}{4},k-\frac{1}{2},h+\frac{1}{4}}^{n-\frac{1}{2}} \Bigg\} \\
= & -i \left(a_x\, p_{x,j+\frac{1}{10}} + a_y\, p_{y,k-\frac{3}{10}} + a_z\, p_{z,h+\frac{1}{10}} \right) \\
& \times \left[\tilde{u} - \frac{3}{20}\tilde{u}_{\bar{p}_x} + \frac{1}{5}\tilde{u}_{\bar{p}_y} - \frac{3}{20}\tilde{u}_{\bar{p}_z} + \frac{\Delta t}{4}\tilde{u}_t \right]_{j+\frac{1}{4},k-\frac{1}{2},h+\frac{1}{4}}^{n-\frac{1}{2}} \Delta V \frac{\Delta t}{2},
\end{aligned}
\tag{4.16}
$$

respectively.

(b) The CEs according to the mesh point $(j_d-\frac{1}{4}, k_d, h_d-\frac{1}{4}, n_d)$, or $(j_d+\frac{3}{4}, k_d, h_d+\frac{3}{4}, n_d)$, or $(j_d+\frac{3}{4}, k_d+1, h_d-\frac{1}{4}, n_d-\frac{1}{2})$, or $(j_d-\frac{1}{4}, k_d+1, h_d+\frac{3}{4}, n_d-\frac{1}{2})$, denoted by $\mathrm{G}(j,k,h)$ are shown in Fig. 4.6. Consider the spatial projections of CEs GBCDE, GABDF, GABCH and GACDI in Fig. 4.6, in which the spatial projections of mesh points E, F, H, I can be denoted by $(j+\frac{1}{2}, k, h)$, $(j, k, h+\frac{1}{2})$, $(j-\frac{1}{4}, k-\frac{1}{2}, h-\frac{1}{4})$, $(j-\frac{1}{4}, k+\frac{1}{2}, h-\frac{1}{4})$, respectively. And then the spatial centroids of these CEs are denoted by $(j+\frac{1}{4}, k, h-\frac{1}{20})$, $(j-\frac{1}{20}, k, h+\frac{1}{4})$, $(j-\frac{1}{10}, k-\frac{3}{10}, h-\frac{1}{10})$, $(j-\frac{1}{10}, k+\frac{3}{10}, h-\frac{1}{10})$, respectively. Thus the

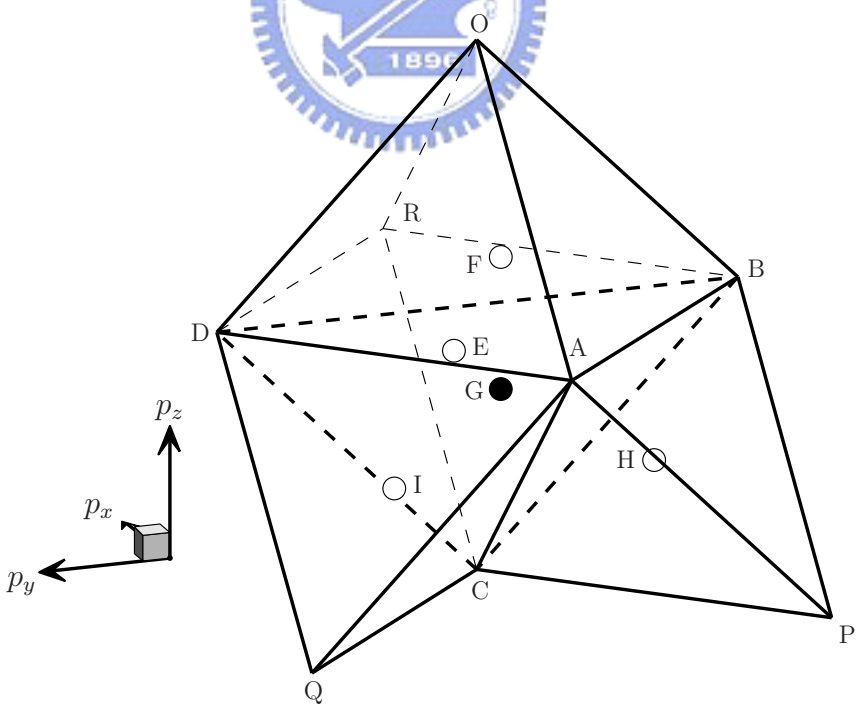

Figure 4.6. Spatial building block (b) in E_4.

approximations of the total flux leaving the boundaries of CEs GBCDE (denoted by CE_1), GABDF (denoted by CE_2), GABCH (denoted by CE_3) and GACDI (denoted by CE_4) in

Fig. 4.6 are

$$\begin{aligned} F_{\mathrm{CE}_1}(j,k,h,n) &= \Delta V \left\{ \left[\tilde{u} + \frac{1}{4}\tilde{u}_{\bar{p}_x} - \frac{1}{20}\tilde{u}_{\bar{p}_z} \right]_{j,k,h}^{n} - \left[\tilde{u} - \frac{1}{4}\tilde{u}_{\bar{p}_x} - \frac{1}{20}\tilde{u}_{\bar{p}_z} \right]_{j+\frac{1}{2},k,h}^{n-\frac{1}{2}} \right\} \\ &= -i \left(a_x\, p_{x,j+\frac{1}{4}} + a_y\, p_{y,k} + a_z\, p_{z,h-\frac{1}{20}} \right) \\ &\quad \times \left[\tilde{u} - \frac{1}{4}\tilde{u}_{\bar{p}_x} - \frac{1}{20}\tilde{u}_{\bar{p}_z} + \frac{\Delta t}{4}\tilde{u}_t \right]_{j+\frac{1}{2},k,h}^{n-\frac{1}{2}} \Delta V \frac{\Delta t}{2}, \end{aligned} \tag{4.17}$$

$$\begin{aligned} F_{\mathrm{CE}_2}(j,k,h,n) &= \Delta V \left\{ \left[\tilde{u} - \frac{1}{20}\tilde{u}_{\bar{p}_x} + \frac{1}{4}\tilde{u}_{\bar{p}_z} \right]_{j,k,h}^{n} - \left[\tilde{u} - \frac{1}{20}\tilde{u}_{\bar{p}_x} - \frac{1}{4}\tilde{u}_{\bar{p}_z} \right]_{j,k,h+\frac{1}{2}}^{n-\frac{1}{2}} \right\} \\ &= -i \left(a_x\, p_{x,j-\frac{1}{20}} + a_y\, p_{y,k} + a_z\, p_{z,h+\frac{1}{4}} \right) \\ &\quad \times \left[\tilde{u} - \frac{1}{20}\tilde{u}_{\bar{p}_x} - \frac{1}{4}\tilde{u}_{\bar{p}_z} + \frac{\Delta t}{4}\tilde{u}_t \right]_{j,k,h+\frac{1}{2}}^{n-\frac{1}{2}} \Delta V \frac{\Delta t}{2}, \end{aligned} \tag{4.18}$$

$$\begin{aligned} F_{\mathrm{CE}_3}(j,k,h,n) &= \Delta V \Bigg\{ \left[\tilde{u} - \frac{1}{10}\tilde{u}_{\bar{p}_x} - \frac{3}{10}\tilde{u}_{\bar{p}_y} - \frac{1}{10}\tilde{u}_{\bar{p}_z} \right]_{j,k,h}^{n} \\ &\quad - \left[\tilde{u} + \frac{3}{20}\tilde{u}_{\bar{p}_x} + \frac{1}{5}\tilde{u}_{\bar{p}_y} + \frac{3}{20}\tilde{u}_{\bar{p}_z} \right]_{j-\frac{1}{4},k-\frac{1}{2},h-\frac{1}{4}}^{n-\frac{1}{2}} \Bigg\} \\ &= -i \left(a_x\, p_{x,j-\frac{1}{10}} + a_y\, p_{y,k-\frac{3}{10}} + a_z\, p_{z,h-\frac{1}{10}} \right) \\ &\quad \times \left[\tilde{u} + \frac{3}{20}\tilde{u}_{\bar{p}_x} + \frac{1}{5}\tilde{u}_{\bar{p}_y} + \frac{3}{20}\tilde{u}_{\bar{p}_z} + \frac{\Delta t}{4}\tilde{u}_t \right]_{j-\frac{1}{4},k-\frac{1}{2},h-\frac{1}{4}}^{n-\frac{1}{2}} \Delta V \frac{\Delta t}{2} \end{aligned} \tag{4.19}$$

and

$$\begin{aligned} F_{\mathrm{CE}_4}(j,k,h,n) &= \Delta V \Bigg\{ \left[\tilde{u} - \frac{1}{10}\tilde{u}_{\bar{p}_x} + \frac{3}{10}\tilde{u}_{\bar{p}_y} - \frac{1}{10}\tilde{u}_{\bar{p}_z} \right]_{j,k,h}^{n} \\ &\quad - \left[\tilde{u} + \frac{3}{20}\tilde{u}_{\bar{p}_x} - \frac{1}{5}\tilde{u}_{\bar{p}_y} + \frac{3}{20}\tilde{u}_{\bar{p}_z} \right]_{j-\frac{1}{4},k+\frac{1}{2},h-\frac{1}{4}}^{n-\frac{1}{2}} \Bigg\} \\ &= -i \left(a_x\, p_{x,j-\frac{1}{10}} + a_y\, p_{y,k+\frac{3}{10}} + a_z\, p_{z,h-\frac{1}{10}} \right) \\ &\quad \times \left[\tilde{u} + \frac{3}{20}\tilde{u}_{\bar{p}_x} - \frac{1}{5}\tilde{u}_{\bar{p}_y} + \frac{3}{20}\tilde{u}_{\bar{p}_z} + \frac{\Delta t}{4}\tilde{u}_t \right]_{j-\frac{1}{4},k+\frac{1}{2},h-\frac{1}{4}}^{n-\frac{1}{2}} \Delta V \frac{\Delta t}{2}, \end{aligned} \tag{4.20}$$

respectively.

(c) The CEs according to the mesh point $(j_d-\frac{3}{4}, k_d-1, h_d-\frac{1}{4}, n_d)$, or $(j_d+\frac{1}{4}, k_d-1, h_d+\frac{3}{4}, n_d)$, or $(j_d+\frac{1}{4}, k_d, h_d-\frac{1}{4}, n_d-\frac{1}{2})$, or $(j_d-\frac{3}{4}, k_d, h_d+\frac{3}{4}, n_d-\frac{1}{2})$, denoted by $\mathrm{G}(j,k,h,n)$ are shown in Fig. 4.7. Consider the spatial projections of CEs GBCDE, GABDF, GABCH and GACDI in Fig. 4.7, in which the spatial projections of mesh points E, F, H, I can be denoted by $(j-\frac{1}{2}, k, h)$, $(j, k, h+\frac{1}{2})$, $(j+\frac{1}{4}, k+\frac{1}{2}, h-\frac{1}{4})$, $(j+\frac{1}{4}, k-\frac{1}{2}, h-\frac{1}{4})$, respectively. And then the spatial centroids of these CEs are denoted by $(j-\frac{1}{4}, k, h-\frac{1}{20})$,

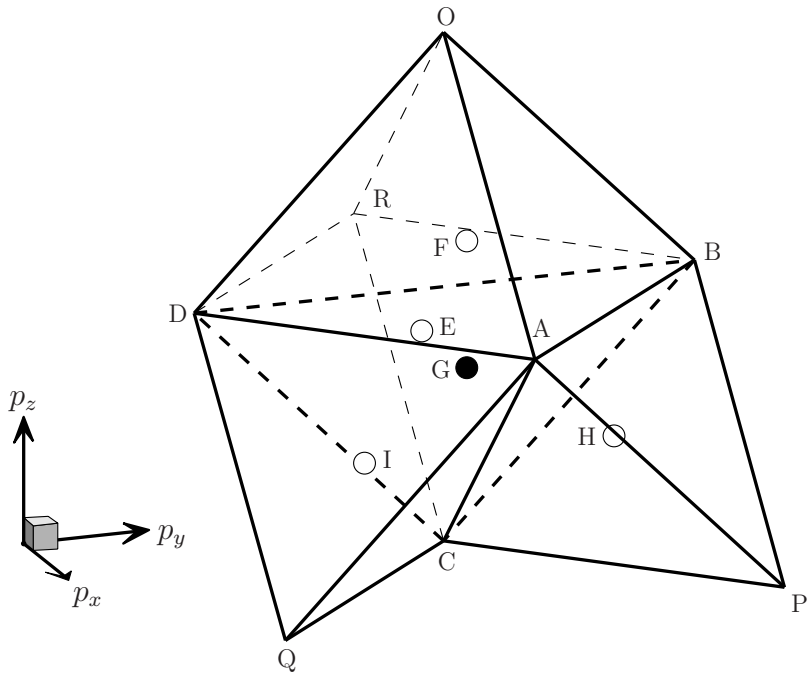

Figure 4.7. Spatial building block (c) in E_4.

$(j+\frac{1}{20},k,h+\frac{1}{4})$, $(j+\frac{1}{10},k+\frac{3}{10},h-\frac{1}{10})$, $(j+\frac{1}{10},k-\frac{3}{10},h-\frac{1}{10})$, respectively. Thus the approximations of the total flux leaving the boundaries of CEs GBCDE (denoted by CE_1), GABDF (denoted by CE_2), GABCH (denoted by CE_3) and GACDI (denoted by CE_4) in Fig. 4.7 are

$$\begin{aligned} F_{\mathrm{CE}_1}(j,k,h,n) &= \Delta V \left\{ \left[\tilde{u} - \frac{1}{4}\tilde{u}_{\bar{p}_x} - \frac{1}{20}\tilde{u}_{\bar{p}_z} \right]_{j,k,h}^{n} - \left[\tilde{u} + \frac{1}{4}\tilde{u}_{\bar{p}_x} - \frac{1}{20}\tilde{u}_{\bar{p}_z} \right]_{j-\frac{1}{2},k,h}^{n-\frac{1}{2}} \right\} \\ &= -i \left(a_x\, p_{x,j-\frac{1}{4}} + a_y\, p_{y,k} + a_z\, p_{z,h-\frac{1}{20}} \right) \\ &\quad \times \left[\tilde{u} + \frac{1}{4}\tilde{u}_{\bar{p}_x} - \frac{1}{20}\tilde{u}_{\bar{p}_z} + \frac{\Delta t}{4}\tilde{u}_t \right]_{j-\frac{1}{2},k,h}^{n-\frac{1}{2}} \Delta V \frac{\Delta t}{2}, \end{aligned} \tag{4.21}$$

$$\begin{aligned} F_{\mathrm{CE}_2}(j,k,h,n) &= \Delta V \left\{ \left[\tilde{u} + \frac{1}{20}\tilde{u}_{\bar{p}_x} + \frac{1}{4}\tilde{u}_{\bar{p}_z} \right]_{j,k,h}^{n} - \left[\tilde{u} + \frac{1}{20}\tilde{u}_{\bar{p}_x} - \frac{1}{4}\tilde{u}_{\bar{p}_z} \right]_{j,k,h+\frac{1}{2}}^{n-\frac{1}{2}} \right\} \\ &= -i \left(a_x\, p_{x,j+\frac{1}{20}} + a_y\, p_{y,k} + a_z\, p_{z,h+\frac{1}{4}} \right) \\ &\quad \times \left[\tilde{u} + \frac{1}{20}\tilde{u}_{\bar{p}_x} - \frac{1}{4}\tilde{u}_{\bar{p}_z} + \frac{\Delta t}{4}\tilde{u}_t \right]_{j,k,h+\frac{1}{2}}^{n-\frac{1}{2}} \Delta V \frac{\Delta t}{2}, \end{aligned} \tag{4.22}$$

$$
\begin{aligned}
F_{\mathrm{CE}_3}(j,k,h,n) = \Delta V \Bigg\{ & \left[\tilde{u} + \frac{1}{10}\tilde{u}_{\bar{p}_x} + \frac{3}{10}\tilde{u}_{\bar{p}_y} - \frac{1}{10}\tilde{u}_{\bar{p}_z}\right]^{n}_{j,k,h} \\
& - \left[\tilde{u} - \frac{3}{20}\tilde{u}_{\bar{p}_x} - \frac{1}{5}\tilde{u}_{\bar{p}_y} + \frac{3}{20}\tilde{u}_{\bar{p}_z}\right]^{n-\frac{1}{2}}_{j+\frac{1}{4},k+\frac{1}{2},h-\frac{1}{4}} \Bigg\} \\
= & -i\left(a_x\, p_{x,j+\frac{1}{10}} + a_y\, p_{y,k+\frac{3}{10}} + a_z\, p_{z,h-\frac{1}{10}}\right) \\
& \times \left[\tilde{u} - \frac{3}{20}\tilde{u}_{\bar{p}_x} - \frac{1}{5}\tilde{u}_{\bar{p}_y} + \frac{3}{20}\tilde{u}_{\bar{p}_z} + \frac{\Delta t}{4}\tilde{u}_t\right]^{n-\frac{1}{2}}_{j+\frac{1}{4},k+\frac{1}{2},h-\frac{1}{4}} \Delta V \frac{\Delta t}{2}
\end{aligned}
\tag{4.23}
$$

and

$$
\begin{aligned}
F_{\mathrm{CE}_4}(j,k,h,n) = \Delta V \Bigg\{ & \left[\tilde{u} + \frac{1}{10}\tilde{u}_{\bar{p}_x} - \frac{3}{10}\tilde{u}_{\bar{p}_y} - \frac{1}{10}\tilde{u}_{\bar{p}_z}\right]^{n}_{j,k,h} \\
& - \left[\tilde{u} - \frac{3}{20}\tilde{u}_{\bar{p}_x} + \frac{1}{5}\tilde{u}_{\bar{p}_y} + \frac{3}{20}\tilde{u}_{\bar{p}_z}\right]^{n-\frac{1}{2}}_{j+\frac{1}{4},k-\frac{1}{2},h-\frac{1}{4}} \Bigg\} \\
= & -i\left(a_x\, p_{x,j+\frac{1}{10}} + a_y\, p_{y,k-\frac{3}{10}} + a_z\, p_{z,h-\frac{1}{10}}\right) \\
& \times \left[\tilde{u} - \frac{3}{20}\tilde{u}_{\bar{p}_x} + \frac{1}{5}\tilde{u}_{\bar{p}_y} + \frac{3}{20}\tilde{u}_{\bar{p}_z} + \frac{\Delta t}{4}\tilde{u}_t\right]^{n-\frac{1}{2}}_{j+\frac{1}{4},k-\frac{1}{2},h-\frac{1}{4}} \Delta V \frac{\Delta t}{2},
\end{aligned}
\tag{4.24}
$$

respectively.

(d) The CEs according to the mesh point $(j_d-\frac{1}{4}, k_d-1, h_d-\frac{3}{4}, n_d)$, or $(j_d+\frac{3}{4}, k_d-1, h_d+\frac{1}{4}, n_d)$, or $(j_d+\frac{3}{4}, k_d, h_d-\frac{3}{4}, n_d-\frac{1}{2})$, or $(j_d-\frac{1}{4}, k_d, h_d+\frac{1}{4}, n_d-\frac{1}{2})$, denoted by $\mathrm{G}(j,k,h,n)$ are shown in Fig. 4.8. Consider the spatial projections of CEs GBCDE, GABDF, GABCH and GACDI in Fig. 4.8, in which the spatial projections of mesh points G, E, F, H, I can be denoted by $(j+\frac{1}{2}, k, h)$, $(j, k, h-\frac{1}{2})$, $(j-\frac{1}{4}, k-\frac{1}{2}, h+\frac{1}{4})$, $(j-\frac{1}{4}, k+\frac{1}{2}, h+\frac{1}{4})$, respectively. And then the spatial centroids of these CEs are denoted by $(j+\frac{1}{4}, k, h+\frac{1}{20})$, $(j-\frac{1}{20}, k, h-\frac{1}{4})$, $(j-\frac{1}{10}, k-\frac{3}{10}, h+\frac{1}{10})$, $(j-\frac{1}{10}, k+\frac{3}{10}, h+\frac{1}{10})$, respectively.

Thus the approximations of the total flux leaving the boundaries of CEs GBCDE (denoted by CE_1), GABDF (denoted by CE_2), GABCH (denoted by CE_3) and GACDI (denoted by CE_4) in Fig. 4.8 are

$$
\begin{aligned}
F_{\mathrm{CE}_1}(j,k,h,n) = \Delta V & \left\{ \left[\tilde{u} + \frac{1}{4}\tilde{u}_{\bar{p}_x} + \frac{1}{20}\tilde{u}_{\bar{p}_z}\right]^{n}_{j,k,h} - \left[\tilde{u} - \frac{1}{4}\tilde{u}_{\bar{p}_x} + \frac{1}{20}\tilde{u}_{\bar{p}_z}\right]^{n-\frac{1}{2}}_{j+\frac{1}{2},k,h} \right\} \\
= & -i\left(a_x\, p_{x,j+\frac{1}{4}} + a_y\, p_{y,k} + a_z\, p_{z,h+\frac{1}{20}}\right) \\
& \times \left[\tilde{u} - \frac{1}{4}\tilde{u}_{\bar{p}_x} + \frac{1}{20}\tilde{u}_{\bar{p}_z} + \frac{\Delta t}{4}\tilde{u}_t\right]^{n-\frac{1}{2}}_{j-\frac{1}{2},k,h} \Delta V \frac{\Delta t}{2},
\end{aligned}
\tag{4.25}
$$

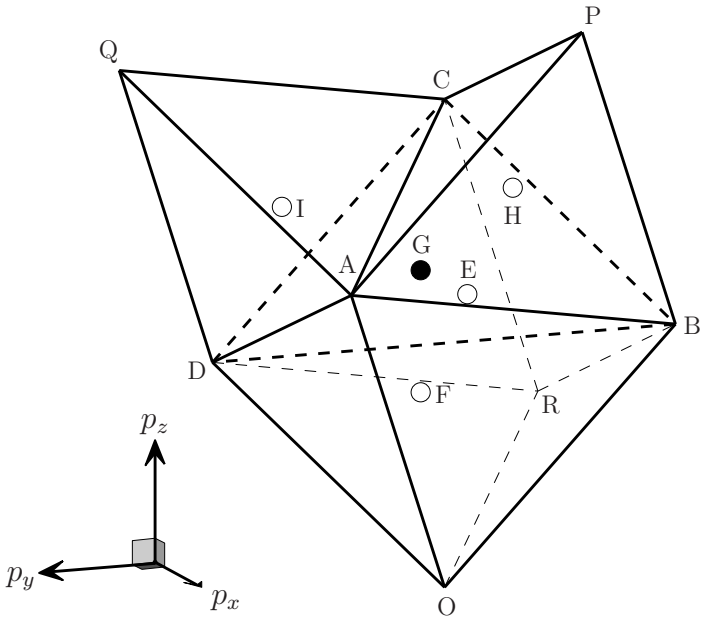

Figure 4.8. Spatial building block (d) in E_4.

$$
\begin{aligned}
F_{\mathrm{CE}_2}(j,k,h,n) &= \Delta V \left\{ \left[\tilde{u} - \frac{1}{20}\tilde{u}_{\bar{p}_x} - \frac{1}{4}\tilde{u}_{\bar{p}_z} \right]_{j,k,h}^{n} - \left[\tilde{u} - \frac{1}{20}\tilde{u}_{\bar{p}_x} + \frac{1}{4}\tilde{u}_{\bar{p}_z} \right]_{j,k,h-\frac{1}{2}}^{n-\frac{1}{2}} \right\} \\
&= -i \left(a_x\, p_{x,j-\frac{1}{20}} + a_y\, p_{y,k} + a_z\, p_{z,h-\frac{1}{4}} \right) \\
&\quad \times \left[\tilde{u} - \frac{1}{20}\tilde{u}_{\bar{p}_x} + \frac{1}{4}\tilde{u}_{\bar{p}_z} + \frac{\Delta t}{4}\tilde{u}_t \right]_{j,k,h-\frac{1}{2}}^{n-\frac{1}{2}} \Delta V \frac{\Delta t}{2},
\end{aligned} \tag{4.26}
$$

$$
\begin{aligned}
F_{\mathrm{CE}_3}(j,k,h,n) &= \Delta V \left\{ \left[\tilde{u} - \frac{1}{10}\tilde{u}_{\bar{p}_x} - \frac{3}{10}\tilde{u}_{\bar{p}_y} + \frac{1}{10}\tilde{u}_{\bar{p}_z} \right]_{j,k,h}^{n} \right. \\
&\quad \left. - \left[\tilde{u} + \frac{3}{20}\tilde{u}_{\bar{p}_x} + \frac{1}{5}\tilde{u}_{\bar{p}_y} - \frac{3}{20}\tilde{u}_{\bar{p}_z} \right]_{j-\frac{1}{4},k-\frac{1}{2},h+\frac{1}{4}}^{n-\frac{1}{2}} \right\} \\
&= -i \left(a_x\, p_{x,j-\frac{1}{10}} + a_y\, p_{y,k-\frac{3}{10}} + a_z\, p_{z,h+\frac{1}{10}} \right) \\
&\quad \times \left[\tilde{u} + \frac{3}{20}\tilde{u}_{\bar{p}_x} + \frac{1}{5}\tilde{u}_{\bar{p}_y} - \frac{3}{20}\tilde{u}_{\bar{p}_z} + \frac{\Delta t}{4}\tilde{u}_t \right]_{j-\frac{1}{4},k-\frac{1}{2},h+\frac{1}{4}}^{n-\frac{1}{2}} \Delta V \frac{\Delta t}{2}
\end{aligned} \tag{4.27}
$$

and

$$
\begin{aligned}
F_{\mathrm{CE}_4}(j,k,h,n) &= \Delta V \left\{ \left[\tilde{u} - \frac{1}{10}\tilde{u}_{\bar{p}_x} + \frac{3}{10}\tilde{u}_{\bar{p}_y} + \frac{1}{10}\tilde{u}_{\bar{p}_z} \right]_{j,k,h}^{n} \right. \\
&\quad \left. - \left[\tilde{u} + \frac{3}{20}\tilde{u}_{\bar{p}_x} - \frac{1}{5}\tilde{u}_{\bar{p}_y} - \frac{3}{20}\tilde{u}_{\bar{p}_z} \right]_{j-\frac{1}{4},k+\frac{1}{2},h+\frac{1}{4}}^{n-\frac{1}{2}} \right\} \\
&= -i \left(a_x\, p_{x,j-\frac{1}{10}} + a_y\, p_{y,k+\frac{3}{10}} + a_z\, p_{z,h+\frac{1}{10}} \right) \\
&\quad \times \left[\tilde{u} + \frac{3}{20}\tilde{u}_{\bar{p}_x} - \frac{1}{5}\tilde{u}_{\bar{p}_y} - \frac{3}{20}\tilde{u}_{\bar{p}_z} + \frac{\Delta t}{4}\tilde{u}_t \right]_{j-\frac{1}{4},k+\frac{1}{2},h+\frac{1}{4}}^{n-\frac{1}{2}} \Delta V \frac{\Delta t}{2},
\end{aligned} \tag{4.28}
$$

respectively.

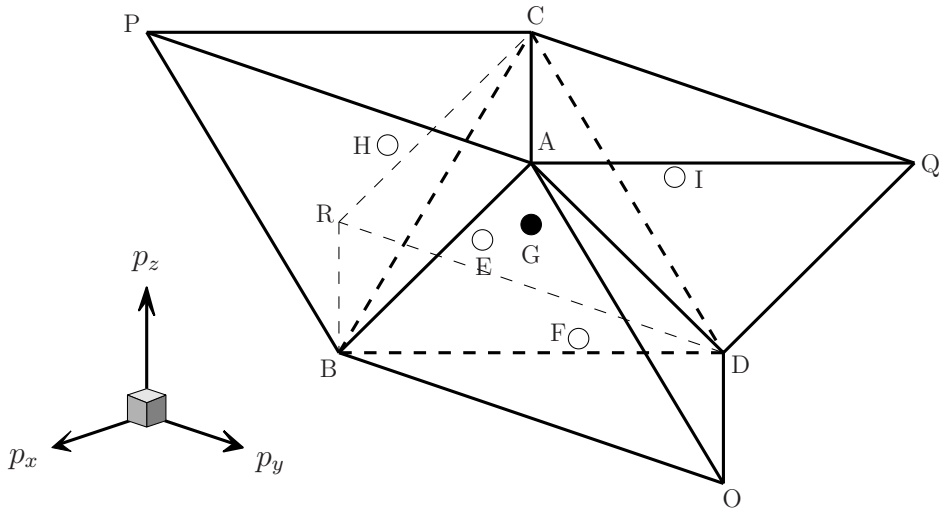

Figure 4.9. Spatial building block (e) in E_4.

(e) The CEs according to the mesh point $(j_d+\frac{1}{2}, k_d-\frac{1}{2}, h_d-\frac{1}{2}, n_d)$, or $(j_d-\frac{1}{2}, k_d-\frac{1}{2}, h_d+\frac{1}{2}, n_d)$, or $(j_d-\frac{1}{2}, k_d+\frac{1}{2}, h_d-\frac{1}{2}, n_d-\frac{1}{2})$, or $(j_d+\frac{1}{2}, k_d+\frac{1}{2}, h_d+\frac{1}{2}, n_d-\frac{1}{2})$, denoted by $\mathrm{G}(j,k,h,n)$ are shown in Fig. 4.9. Consider the spatial projections of CEs GBCDE, GABDF, GABCH and GACDI in Fig. 4.9, in which the spatial projections of mesh points G, E, F, H, I can be denoted by $(j-\frac{1}{4}, k-\frac{1}{2}, h-\frac{1}{4})$, $(j+\frac{1}{4}, k+\frac{1}{2}, h-\frac{1}{4})$, $(j+\frac{1}{4}, k-\frac{1}{2}, h+\frac{1}{4})$, $(j-\frac{1}{4}, k+\frac{1}{2}, h+\frac{1}{4})$, respectively. And then the spatial centroids of these CEs are denoted by $(j-\frac{3}{20}, k-\frac{1}{5}, h-\frac{3}{20})$, $(j+\frac{3}{20}, k+\frac{1}{5}, h-\frac{3}{20})$, $(j+\frac{3}{20}, k-\frac{1}{5}, h+\frac{3}{20})$, $(j-\frac{3}{20}, k+\frac{1}{5}, h+\frac{3}{20})$, respectively.

Thus the approximations of the total flux leaving the boundaries of CEs GBCDE (denoted by CE_1), GABDF (denoted by CE_2), GABCH (denoted by CE_3) and GACDI (denoted by CE_4) in Fig. 4.9 are

$$\begin{aligned} F_{\mathrm{CE}_1}(j,k,h,n) = \Delta V \Bigg\{ & \left[\tilde{u} - \frac{3}{20}\tilde{u}_{\bar{p}_x} - \frac{1}{5}\tilde{u}_{\bar{p}_y} - \frac{3}{20}\tilde{u}_{\bar{p}_z}\right]_{j,k,h}^{n} \\ & - \left[\tilde{u} + \frac{1}{10}\tilde{u}_{\bar{p}_x} + \frac{3}{10}\tilde{u}_{\bar{p}_y} + \frac{1}{10}\tilde{u}_{\bar{p}_z}\right]_{j-\frac{1}{4},k-\frac{1}{2},h-\frac{1}{4}}^{n-\frac{1}{2}} \Bigg\} \\ = {} & -i\,\Delta V \frac{\Delta t}{2}\left(a_x\, p_{x,j-\frac{3}{20}} + a_y\, p_{y,k-\frac{1}{5}} + a_z\, p_{z,h-\frac{3}{20}}\right) \\ & \times \left[\tilde{u} + \frac{1}{10}\tilde{u}_{\bar{p}_x} + \frac{3}{10}\tilde{u}_{\bar{p}_y} + \frac{1}{10}\tilde{u}_{\bar{p}_z} + \frac{\Delta t}{4}\tilde{u}_t\right]_{j-\frac{1}{4},k-\frac{1}{2},h-\frac{1}{4}}^{n-\frac{1}{2}}, \end{aligned} \tag{4.29}$$

$$
\begin{aligned}
F_{\mathrm{CE}_2}(j,k,h,n) &= \Delta V \Bigg\{ \left[\tilde{u} + \frac{3}{20}\tilde{u}_{\bar{p}_x} + \frac{1}{5}\tilde{u}_{\bar{p}_y} - \frac{3}{20}\tilde{u}_{\bar{p}_z} \right]_{j,k,h}^{n} \\
&\quad - \left[\tilde{u} - \frac{1}{10}\tilde{u}_{\bar{p}_x} - \frac{3}{10}\tilde{u}_{\bar{p}_y} + \frac{1}{10}\tilde{u}_{\bar{p}_z} \right]_{j+\frac{1}{4},k+\frac{1}{2},h-\frac{1}{4}}^{n-\frac{1}{2}} \Bigg\} \\
&= -i\,\Delta V \frac{\Delta t}{2} \left(a_x\, p_{x,j+\frac{3}{20}} + a_y\, p_{y,k+\frac{1}{5}} + a_z\, p_{z,h-\frac{3}{20}} \right) \\
&\quad \times \left[\tilde{u} - \frac{1}{10}\tilde{u}_{\bar{p}_x} - \frac{3}{10}\tilde{u}_{\bar{p}_y} + \frac{1}{10}\tilde{u}_{\bar{p}_z} + \frac{\Delta t}{4}\tilde{u}_t \right]_{j+\frac{1}{4},k+\frac{1}{2},h-\frac{1}{4}}^{n-\frac{1}{2}},
\end{aligned}
\tag{4.30}
$$

$$
\begin{aligned}
F_{\mathrm{CE}_3}(j,k,h,n) &= \Delta V \Bigg\{ \left[\tilde{u} + \frac{3}{20}\tilde{u}_{\bar{p}_x} - \frac{1}{5}\tilde{u}_{\bar{p}_y} + \frac{3}{20}\tilde{u}_{\bar{p}_z} \right]_{j,k,h}^{n} \\
&\quad - \left[\tilde{u} - \frac{1}{10}\tilde{u}_{\bar{p}_x} + \frac{3}{10}\tilde{u}_{\bar{p}_y} - \frac{1}{10}\tilde{u}_{\bar{p}_z} \right]_{j+\frac{1}{4},k-\frac{1}{2},h+\frac{1}{4}}^{n-\frac{1}{2}} \Bigg\} \\
&= -i\,\Delta V \frac{\Delta t}{2} \left(a_x\, p_{x,j+\frac{3}{20}} + a_y\, p_{y,k-\frac{1}{5}} + a_z\, p_{z,h+\frac{3}{20}} \right) \\
&\quad \times \left[\tilde{u} - \frac{1}{10}\tilde{u}_{\bar{p}_x} + \frac{3}{10}\tilde{u}_{\bar{p}_y} - \frac{1}{10}\tilde{u}_{\bar{p}_z} + \frac{\Delta t}{4}\tilde{u}_t \right]_{j+\frac{1}{4},k-\frac{1}{2},h+\frac{1}{4}}^{n-\frac{1}{2}}
\end{aligned}
\tag{4.31}
$$

and

$$
\begin{aligned}
F_{\mathrm{CE}_4}(j,k,h,n) &= \Delta V \Bigg\{ \left[\tilde{u} - \frac{3}{20}\tilde{u}_{\bar{p}_x} + \frac{1}{5}\tilde{u}_{\bar{p}_y} + \frac{3}{20}\tilde{u}_{\bar{p}_z} \right]_{j,k,h}^{n} \\
&\quad - \left[\tilde{u} + \frac{1}{10}\tilde{u}_{\bar{p}_x} - \frac{3}{10}\tilde{u}_{\bar{p}_y} - \frac{1}{10}\tilde{u}_{\bar{p}_z} \right]_{j-\frac{1}{4},k+\frac{1}{2},h+\frac{1}{4}}^{n-\frac{1}{2}} \Bigg\} \\
&= -i\,\Delta V \frac{\Delta t}{2} \left(a_x\, p_{x,j-\frac{3}{20}} + a_y\, p_{y,k+\frac{1}{5}} + a_z\, p_{z,h+\frac{3}{20}} \right) \\
&\quad \times \left[\tilde{u} + \frac{1}{10}\tilde{u}_{\bar{p}_x} - \frac{3}{10}\tilde{u}_{\bar{p}_y} - \frac{1}{10}\tilde{u}_{\bar{p}_z} + \frac{\Delta t}{4}\tilde{u}_t \right]_{j-\frac{1}{4},k+\frac{1}{2},h+\frac{1}{4}}^{n-\frac{1}{2}},
\end{aligned}
\tag{4.32}
$$

respectively.

(f) The CEs according to the mesh point $(j_d + \frac{1}{2}, k_d + \frac{1}{2}, h_d - \frac{1}{2}, n_d)$, or $(j_d - \frac{1}{2}, k_d + \frac{1}{2}, h_d + \frac{1}{2}, n_d)$, or $(j_d - \frac{1}{2}, k_d - \frac{1}{2}, h_d - \frac{1}{2}, n_d - \frac{1}{2})$, or $(j_d + \frac{1}{2}, k_d - \frac{1}{2}, h_d + \frac{1}{2}, n_d - \frac{1}{2})$, denoted by $\mathrm{G}(j,k,h,n)$ are shown in Fig. 4.10. Consider the spatial projections of CEs GBCDE, GABDF, GABCH and GACDI in Fig. 4.10, in which the spatial projections of mesh points G, E, F, H, I can be denoted by $(j-\frac{1}{4}, k-\frac{1}{2}, h-\frac{1}{4})$, $(j+\frac{1}{4}, k+\frac{1}{2}, h-\frac{1}{4})$, $(j+\frac{1}{4}, k-\frac{1}{2}, h+\frac{1}{4})$, $(j-\frac{1}{4}, k+\frac{1}{2}, h+\frac{1}{4})$, respectively. And then the spatial centroids of these CEs are denoted by $(j-\frac{3}{20}, k-\frac{1}{5}, h-\frac{3}{20})$, $(j+\frac{3}{20}, k+\frac{1}{5}, h-\frac{3}{20})$, $(j+\frac{3}{20}, k-\frac{1}{5}, h+\frac{3}{20})$, $(j-\frac{3}{20}, k+\frac{1}{5}, h+\frac{3}{20})$, respectively.

Thus the approximations of the total flux leaving the boundaries of CEs GBCDE (denoted by CE_1), GABDF (denoted by CE_2), GABCH (denoted by CE_3) and GACDI

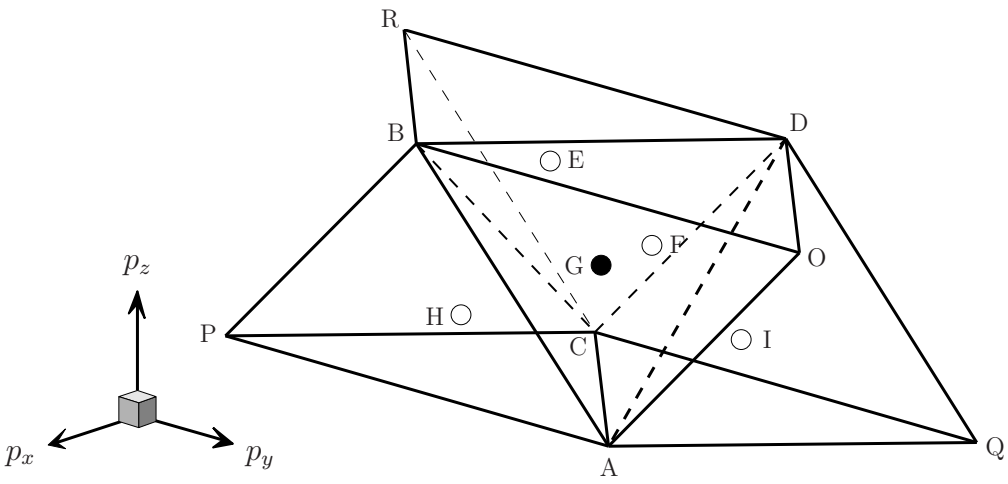

Figure 4.10. Spatial building block (f) in E_4.

(denoted by CE_4) in Fig. 4.10 are

$$\begin{aligned}
F_{\mathrm{CE}_1}(j,k,h,n) &= \Delta V \Bigg\{ \left[\tilde{u} - \frac{3}{20}\tilde{u}_{\bar{p}_x} - \frac{1}{5}\tilde{u}_{\bar{p}_y} + \frac{3}{20}\tilde{u}_{\bar{p}_z} \right]^{n}_{j,k,h} \\
&\quad - \left[\tilde{u} + \frac{1}{10}\tilde{u}_{\bar{p}_x} + \frac{3}{10}\tilde{u}_{\bar{p}_y} - \frac{1}{10}\tilde{u}_{\bar{p}_z} \right]^{n-\frac{1}{2}}_{j-\frac{1}{4},k-\frac{1}{2},h+\frac{1}{4}} \Bigg\} \\
&= -i\,\Delta V \frac{\Delta t}{2} \left(a_x\, p_{x,j-\frac{3}{20}} + a_y\, p_{y,k-\frac{1}{5}} + a_z\, p_{z,h+\frac{3}{20}} \right) \\
&\quad \times \left[\tilde{u} + \frac{1}{10}\tilde{u}_{\bar{p}_x} + \frac{3}{10}\tilde{u}_{\bar{p}_y} - \frac{1}{10}\tilde{u}_{\bar{p}_z} + \frac{\Delta t}{4}\tilde{u}_t \right]^{n-\frac{1}{2}}_{j-\frac{1}{4},k-\frac{1}{2},h+\frac{1}{4}},
\end{aligned} \tag{4.33}$$

$$\begin{aligned}
F_{\mathrm{CE}_2}(j,k,h,n) &= \Delta V \Bigg\{ \left[\tilde{u} + \frac{3}{20}\tilde{u}_{\bar{p}_x} + \frac{1}{5}\tilde{u}_{\bar{p}_y} + \frac{3}{20}\tilde{u}_{\bar{p}_z} \right]^{n}_{j,k,h} \\
&\quad - \left[\tilde{u} - \frac{1}{10}\tilde{u}_{\bar{p}_x} - \frac{3}{10}\tilde{u}_{\bar{p}_y} - \frac{1}{10}\tilde{u}_{\bar{p}_z} \right]^{n-\frac{1}{2}}_{j+\frac{1}{4},k+\frac{1}{2},h+\frac{1}{4}} \Bigg\} \\
&= -i\,\Delta V \frac{\Delta t}{2} \left(a_x\, p_{x,j+\frac{3}{20}} + a_y\, p_{y,k+\frac{1}{5}} + a_z\, p_{z,h+\frac{3}{20}} \right) \\
&\quad \times \left[\tilde{u} - \frac{1}{10}\tilde{u}_{\bar{p}_x} - \frac{3}{10}\tilde{u}_{\bar{p}_y} - \frac{1}{10}\tilde{u}_{\bar{p}_z} + \frac{\Delta t}{4}\tilde{u}_t \right]^{n-\frac{1}{2}}_{j+\frac{1}{4},k+\frac{1}{2},h+\frac{1}{4}},
\end{aligned} \tag{4.34}$$

$$\begin{aligned}
F_{\mathrm{CE}_3}(j,k,h,n) &= \Delta V \Bigg\{ \left[\tilde{u} + \frac{3}{20}\tilde{u}_{\bar{p}_x} - \frac{1}{5}\tilde{u}_{\bar{p}_y} - \frac{3}{20}\tilde{u}_{\bar{p}_z} \right]^{n}_{j,k,h} \\
&\quad - \left[\tilde{u} - \frac{1}{10}\tilde{u}_{\bar{p}_x} + \frac{3}{10}\tilde{u}_{\bar{p}_y} + \frac{1}{10}\tilde{u}_{\bar{p}_z} \right]^{n-\frac{1}{2}}_{j+\frac{1}{4},k-\frac{1}{2},h-\frac{1}{4}} \Bigg\} \\
&= -i\,\Delta V \frac{\Delta t}{2} \left(a_x\, p_{x,j+\frac{3}{20}} + a_y\, p_{y,k-\frac{1}{5}} + a_z\, p_{z,h-\frac{3}{20}} \right) \\
&\quad \times \left[\tilde{u} - \frac{1}{10}\tilde{u}_{\bar{p}_x} + \frac{3}{10}\tilde{u}_{\bar{p}_y} + \frac{1}{10}\tilde{u}_{\bar{p}_z} + \frac{\Delta t}{4}\tilde{u}_t \right]^{n-\frac{1}{2}}_{j+\frac{1}{4},k-\frac{1}{2},h-\frac{1}{4}},
\end{aligned} \tag{4.35}$$

and

$$
\begin{aligned}
F_{\mathrm{CE}_4}(j,k,h,n) = \Delta V \Bigg\{ & \left[\tilde{u} - \frac{3}{20}\tilde{u}_{\bar{p}_x} + \frac{1}{5}\tilde{u}_{\bar{p}_y} - \frac{3}{20}\tilde{u}_{\bar{p}_z} \right]_{j,k,h}^{n} \\
& - \left[\tilde{u} + \frac{1}{10}\tilde{u}_{\bar{p}_x} - \frac{3}{10}\tilde{u}_{\bar{p}_y} + \frac{1}{10}\tilde{u}_{\bar{p}_z} \right]_{j-\frac{1}{4},k+\frac{1}{2},h-\frac{1}{4}}^{n-\frac{1}{2}} \Bigg\} \\
= & -i\,\Delta V \frac{\Delta t}{2} \left(a_x\, p_{x,j-\frac{3}{20}} + a_y\, p_{y,k+\frac{1}{5}} + a_z\, p_{z,h-\frac{3}{20}} \right) \\
& \times \left[\tilde{u} + \frac{1}{10}\tilde{u}_{\bar{p}_x} - \frac{3}{10}\tilde{u}_{\bar{p}_y} + \frac{1}{10}\tilde{u}_{\bar{p}_z} + \frac{\Delta t}{4}\tilde{u}_t \right]_{j-\frac{1}{4},k+\frac{1}{2},h-\frac{1}{4}}^{n-\frac{1}{2}},
\end{aligned}
\tag{4.36}
$$

respectively.

4.3 Numerical Results

Eq. (4.1)

$$
\frac{\partial u}{\partial t} + a_x \frac{\partial u}{\partial x} + a_y \frac{\partial u}{\partial y} = 0 \tag{4.1}
$$

has an exact solution

$$
u_e = \exp\left[-\frac{(x - a_x\, t)^2 + (y - a_y\, t)^2}{2} \right]. \tag{4.37}
$$

By marking Fourier transformation, Eq. (4.37) can be transformed into

$$
\tilde{u}_e = \exp\left[-\frac{(p_x^2 + p_y^2)}{2} - i\,(a_x\, p_x + a_y\, p_y)\, t \right], \tag{4.38}
$$

in this section, we take $a_x = 1$ and $a_y = 1$.

Consider the model problem Eq. (4.2) with the initial values given by Eq. (4.37) at $t = 0$, the numerical results at $t = 5$ are shown in Figs. 4.11 and 4.12.

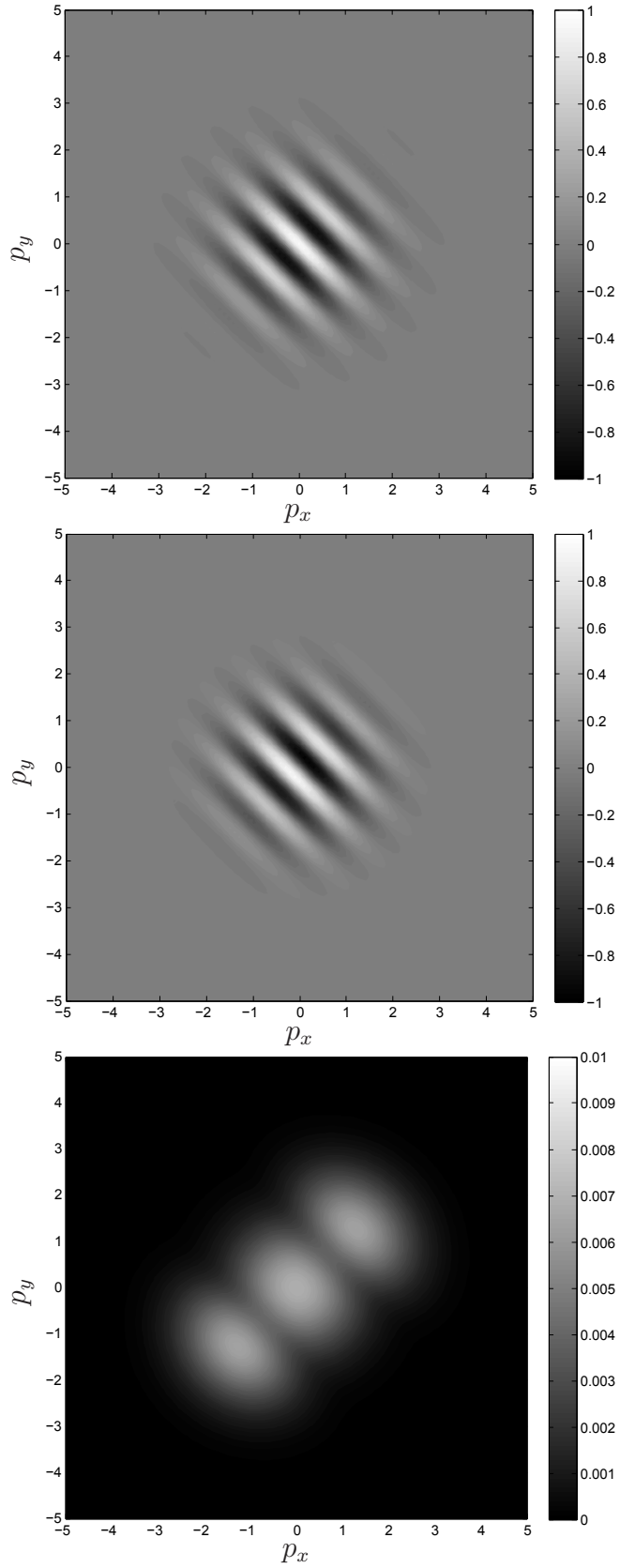

Figure 4.11. Contour plots of the real part, imaginary part of $\tilde{u}$, and $|\tilde{u} - \tilde{u}_e|$ with respect to the $p_x - p_y$ plane. Numerical results at $t = 5$ are obtained with the number of cells of mesh 10^4 in the domain with $p_x \in [-5, 5]$ and $p_y \in [-5, 5]$.

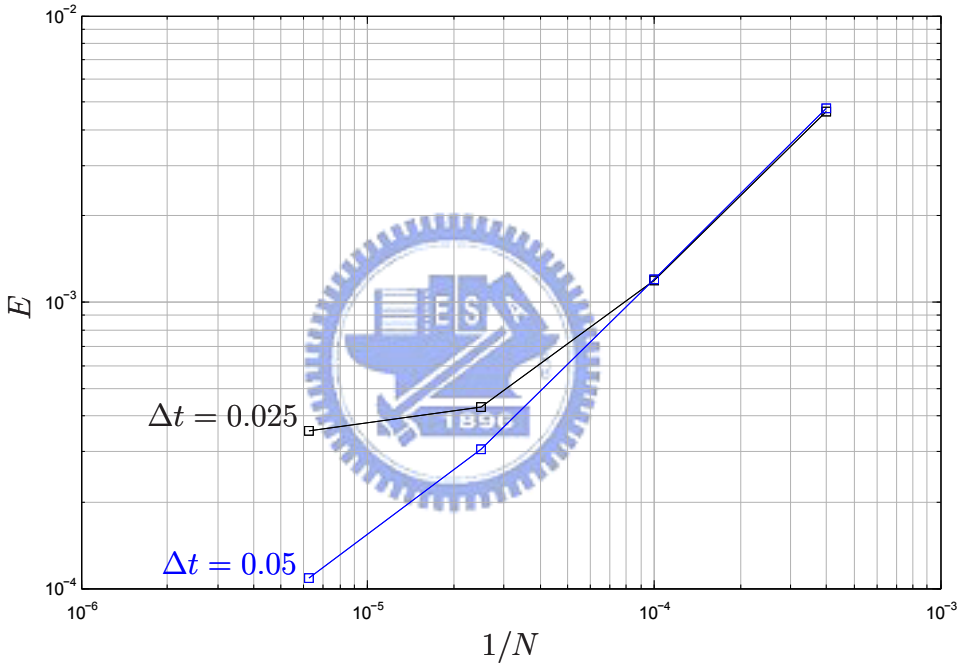

Figure 4.12. Numerical errors with $\Delta t = 0.025$ and 0.05. ($\varepsilon = 10^{-6}$)

For 3D case, consider Eq. (4.10)

$$\frac{\partial u}{\partial t} + a_x \frac{\partial u}{\partial x} + a_y \frac{\partial u}{\partial y} + a_z \frac{\partial u}{\partial z} = 0 \tag{4.10}$$

with an exact solution

$$u_e = \exp\left[-\frac{(x - a_x\, t)^2 + (y - a_y\, t)^2 + (z - a_z\, t)^2}{2} \right]. \tag{4.39}$$

By marking the Fourier transformation, Eq. (4.39) can be transformed into

$$\tilde{u}_e = \exp\left[-\frac{\left(p_x^2 + p_y^2 + p_y^2\right)}{2} - i\,(a_x\, p_x + a_y\, p_y + a_z\, p_z)\, t \right], \tag{4.40}$$

we take $a_x = 1$, $a_y = 1$ and $a_z = 1$ in this section.

For the model problem Eq. (4.11) with the initial values are given by Eq. (4.39) at $t = 0$, the numerical results at $t = 5$ are shown in Fig. 4.13.

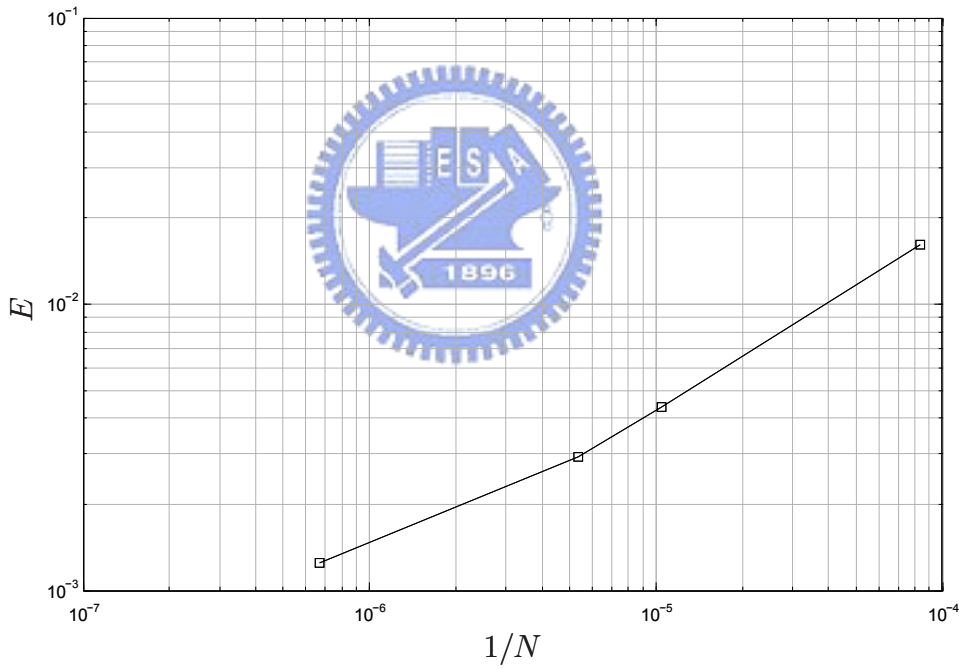

Figure 4.13. Numerical errors with $\Delta t = 0.1$, assuming $p_x \in [-5, 5]$, $p_y \in [-5, 5]$, and $p_z \in [-5, 5]$

Chapter 5

A Quantum Mechanical Problem

5.1 Harmonic Oscillating Charge Interacts with Electromagnetic Wave

The time dependent Schrödinger equation for a simple harmonic oscillated charge q, interacting with electromagnetic wave is written as

$$i\frac{\partial u}{\partial t} = \left[\frac{p^2}{2} + \frac{1}{2}\Omega^2 x^2 - A(t)\cdot p\right] u. \tag{5.1}$$

Throughout this chapter, we take $\hbar = 1$, $m = 1$, and $q = 1$. The relationship between the electric field and vector potential is given by

$$E(t) = -\partial A(t)/\partial t.$$

The transition probability from the ground state $|0>$ to the excited state $|n>$ is given by the Poisson distribution

$$P_{0\to n} = e^{-\sigma}\frac{\sigma^n}{n!}, \tag{5.2}$$

where

$$\sigma = \frac{1}{2\Omega}\left|\int_{\infty}^{\infty} E(t)e^{i\Omega t}\cdot dt\right|^2. \tag{5.3}$$

Recast Eq. (5.1) into p-space we obtain

$$i\,\tilde{u}_t + \frac{1}{2}\,\Omega^2\,\tilde{u}_{pp} = \left[\frac{p^2}{2} - A(t)\cdot p\right]\tilde{u}. \tag{5.4}$$

Requiring that $\tilde{u} = \tilde{u}(p,t;j,n)$ defined by Eq. (3.4) satisfies Eq. (5.4) within SE(j,n), one has

$$(\tilde{u}_t)_j^n = -i\left[\frac{p_j^2}{2} - A(t^n)\cdot p_j\right]\tilde{u}_j^n \tag{5.5}$$

and

$$(\tilde{u}_{pt})_j^n = 0. \tag{5.6}$$

Furthermore, for $(x,t) \in \mathrm{SE}(j,n)$, designate

$$\mathbf{h}(x,t;j,n) = \left(1/2\,\Omega^2\,\tilde{u}_p(x,t;j,n), i\,\tilde{u}(x,t;j,n)\right). \tag{5.7}$$

The approximation of the total flux leaving the boundary of $\mathrm{CE}_{\pm}(j,n)$ is

$$F_{\pm}(j,n) = \oint_{S(\mathrm{CE}_{\pm}(j,n))} \mathbf{h}\cdot d\mathbf{s} = \int_{\mathrm{CE}_{\pm}(j,n)} \left[\frac{p^2}{2} - A(t)\cdot p\right] \tilde{u}\, d\tau \tag{5.8}$$

By Eqs. (5.8), the total flux leaving $\mathrm{CE}_{\pm}(j,n)$ can be derived as

$$\begin{aligned} F_{\pm}(j,n) &= i\frac{\Delta p}{2}\left\{\tilde{u}_j^n \pm \frac{1}{4}(\tilde{u}_{\bar{p}})_j^n - \left[\tilde{u}_{j\pm\frac{1}{2}}^{n-\frac{1}{2}} \mp \frac{1}{4}(\tilde{u}_{\bar{p}})_{j\pm\frac{1}{2}}^{n-\frac{1}{2}}\right]\right\} \\ &\quad \mp \frac{1}{4}\Omega^2\frac{\Delta t}{\Delta p}\left[(\tilde{u}_{\bar{p}})_j^n - (\tilde{u}_{\bar{p}})_{j+\frac{1}{2}}^{n-\frac{1}{2}}\right] \\ &= \frac{\Delta p}{2}\frac{\Delta t}{2}\left[\frac{p_{j\pm\frac{1}{4}}^2}{2} - A(t^{n-\frac{1}{4}})\cdot p_{j\pm\frac{1}{4}}\right] \\ &\quad \times \left[\tilde{u}_{j\pm\frac{1}{2}}^{n-\frac{1}{2}} \mp \frac{1}{4}(\tilde{u}_{\bar{p}})_{j\pm\frac{1}{2}}^{n-\frac{1}{2}} + \frac{\Delta t}{4}(\tilde{u}_t)_{j\pm\frac{1}{2}}^{n-\frac{1}{2}}\right] \end{aligned} \tag{5.9}$$

With the aid of Eqs. (5.5) and (5.9), $\tilde{u}_j^n$ and $(\tilde{u}_{\bar{p}})_j^n$ can be solved in terms of $\tilde{u}_{j\pm1/2}^{n-1/2}$ and $(\tilde{u}_{\bar{p}})_{j\pm1/2}^{n-1/2}$.

5.2 Numerical Results

Consider the model problem Eq. (5.4)

$$i\,\tilde{u}_t + \frac{1}{2}\,\Omega^2\,\tilde{u}_{pp} = \left[\frac{p^2}{2} - A(t)\cdot p\right]\tilde{u} \tag{5.4}$$

Choose a practical Sin^2 pulse,

$$E(t) = E_{amp}\,\sin^2\frac{\pi t}{T}\,\cos\omega t, \tag{5.10}$$

$$0 < t < T.$$

Assume $E_{amp} = 0.002$, the frequency of the electric field $\omega = 0.057$ (wavelength 800 nm) and the total time of pulse T is 8 optical cycles of the carrier wave . Furthermore, we assume the near resonance case, $\Omega = 0.058$ and the initial values are given by ground state

$$\tilde{u}_0 = \frac{1}{(\Omega\,\pi)^{\frac{1}{4}}}\exp\left(-\frac{p^2}{2\,\Omega}\right). \tag{5.11}$$

The results of the transition probability from the ground state to the excited states are shown in Table 5.1. The transition probabilities $P_{0\to N}$ from the ground state to the N-th excited states $\tilde{u}_N$ are derived from

$$P_{0\to N} = \left|\int_{-\infty}^{\infty}\tilde{u}\,\tilde{u}_N\,dp\right|^2. \tag{5.12}$$

Assuming that the computational region of p is defined by from -1.5 to 1.5, the results of $P_{0\to N}$ are shown in Table 5.1.

Table 5.1. Numerical results of $P_{0\to N}$

	$P_{0\to N}$				
		computation result with $\varepsilon = 10^{-6}$			
N	exact solution	4×10^{-4}, 0.01	8×10^{-4}, 0.02	8×10^{-4}, 0.04	8×10^{-4}, 0.08
0	0.1951894	0.1950211	0.1948923	0.1940719	0.1916537
1	0.3188975	0.3185901	0.3183566	0.3168929	0.3130507
2	0.2605050	0.2604394	0.2603970	0.2602243	0.2612223
3	0.1418697	0.1420396	0.1421716	0.1430856	0.1462422
4	0.0579461	0.0581371	0.0582811	0.0591675	0.0609044
5	0.0189343	0.0190470	0.0191296	0.0195836	0.0198997
6	0.0051558	0.0052025	0.0052353	0.0053896	0.0053358
7	0.0012033	0.0012183	0.0012287	0.0012640	0.0012595

noted : 4×10^{-4}, 0.01 denote $\Delta t = 4\times10^{-4}$, and $\Delta p = 0.01$ etc.

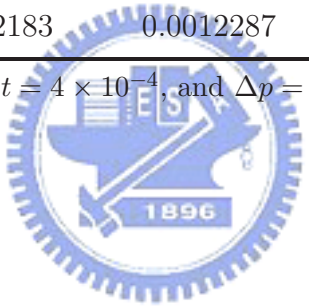

Chapter 6

A Nonlinear Problem

6.1 Example of the KdV Equation

In this chapter, we consider the *Korteweg-de Vries* equation as an example of the nonlinear systems,

$$\frac{1}{\beta}\frac{\partial u}{\partial t} + \frac{\alpha}{\gamma}u\frac{\partial u}{\partial x} + \frac{1}{\gamma^3}\frac{\partial^3 u}{\partial x^3} = 0, \tag{6.1}$$

,where α, β and γ are real (non-zero) constants. The system contains both nonlinearity and dispersion. This is a general form of the KdV equation. For convenience, we study in this chapter

$$u_t + u\,u_x + u_{xxx} = 0 \tag{6.2}$$

By marking the Fourier transformation, the equation can be transformed into the momentum representation

$$\tilde{u}_t = -\frac{1}{2\sqrt{2\pi}}\,i\,p\int_{-\infty}^{\infty}\tilde{u}(q,t)\,\tilde{u}(p-q,t)dq + i\,p^3\,\tilde{u} \tag{6.3}$$

By using Gauss divergence theorem in E_2, Eq. (6.3) can be written as

$$\oint_{S(V)}\mathbf{h}\cdot d\mathbf{s} = \int_V\left[-\frac{1}{2\sqrt{2\pi}}\,i\,p\int_{-\infty}^{\infty}\tilde{u}(q,t)\,\tilde{u}(p-q,t)\,dq + i\,p^3\,\tilde{u}\right]d\tau, \tag{6.4}$$

where $\mathbf{h} = (0, \tilde{u})$.

Requiring that $u = u(p,t;j,n)$ defined by Eq. (3.4) satisfies Eq. (6.3) within SE(j,n), one has

$$(\tilde{u}_t)^n_j = -\frac{1}{2\sqrt{2\pi}}\,i\,p_j\int_{-\infty}^{\infty}\tilde{u}(q,t^n)\,\tilde{u}(p_j-q,t^n)\,dq + i\,p^3\,\tilde{u}^n_j \tag{6.5}$$

The approximation of the total flux leaving the boundary of CE$_\pm(j,n)$ is

$$\begin{aligned} F_\pm &= \oint_{S(\mathrm{CE}_\pm(j,n))}\mathbf{h}(x,t;j,n)\cdot d\mathbf{s} \\ &= -\frac{1}{2\sqrt{2\pi}}\,i\int_{\mathrm{CE}_\pm(j,n)}p\left(\int_{-\infty}^{\infty}\tilde{u}(q,t)\,\tilde{u}(p-q,t)\,dq\right)d\tau \\ &\quad + \int_{\mathrm{CE}_\pm(j,n)}i\,p^3\,\tilde{u}\,d\tau, \end{aligned} \tag{6.6}$$

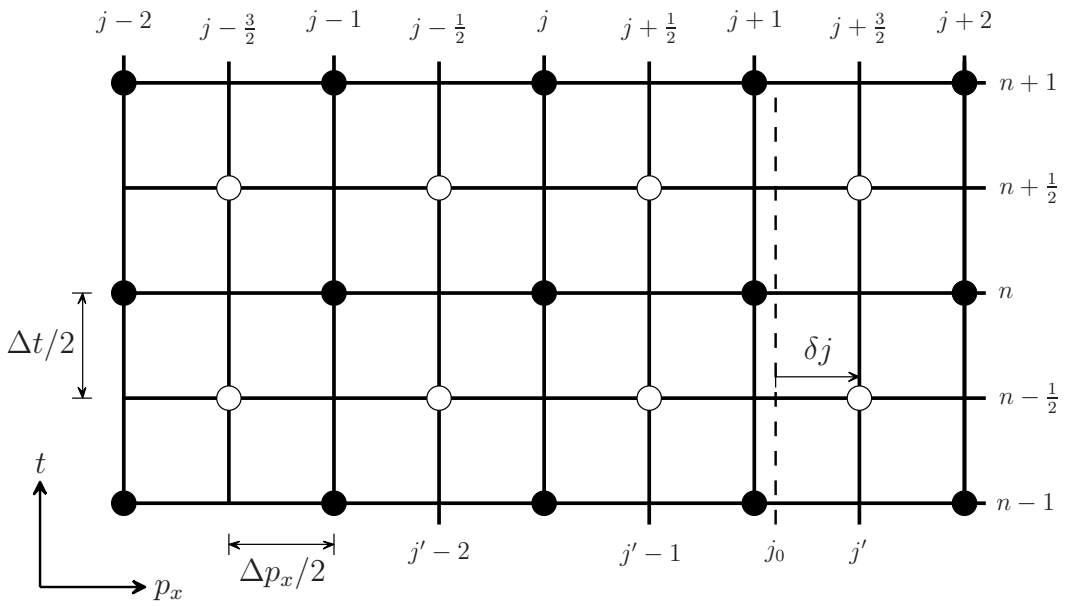

Figure 6.1. Definition of δj

where $\mathbf{h}(p,t;j,n) = (0, \tilde{u}(p,t;j,n))$.

We now approach the subject of the integrand of the first term of the right side of Eq. (6.6), i.e.

$$\int_{-\infty}^{\infty} \tilde{u}(q,t)\,\tilde{u}(p_j - q, t)\,dq. \tag{6.7}$$

It can be approximated as

$$\sum_{\bar{m}} \left[\tilde{u}(q_{\bar{m}},t)\,\tilde{u}(p_j - q_{\bar{m}},t)\right]. \tag{6.8}$$

Let j_0 be the index of $p = 0$ and the index of its nearest mesh point that belongs to the set at $n - \frac{1}{2}$ be j'. Furthermore, we define that $\delta j = j' - j_0$ (see Fig. 6.1). Obviously, $-\frac{1}{2} \le \delta j \le \frac{1}{2}$.

The integral of Eq. (6.6) within $\mathrm{CE}_+(j,n)$ is approximated as

$$\begin{aligned}\int_{\mathrm{CE}_+(j,n)} p\left(\int_{-\infty}^{\infty} \tilde{u}(q,t)\,\tilde{u}(p-q,t)\,dq\right)d\tau = p_{j+\frac{1}{4}}\frac{\Delta p}{2}\frac{\Delta t}{2} \\ \times \sum_m \left\{\left[\tilde{u}_m^{n-\frac{1}{2}} - \frac{1}{4}(\tilde{u}_{\bar{p}})_m^{n-\frac{1}{2}} + \frac{\Delta t}{4}(\tilde{u}_t)_m^{n-\frac{1}{2}}\right]\tilde{u}_{j+\frac{1}{4}-m+j_0}^{n-\frac{1}{4}}\right\},\end{aligned} \tag{6.9}$$

in the above and hereafter, m belongs to the set of mesh points at $n - \frac{1}{2}$.

If $\frac{1}{4} \le \delta j \le \frac{1}{2}$, $\tilde{u}_{j+\frac{1}{4}-m+j_0}^{n-\frac{1}{4}}$ can be approximated as

$$\begin{aligned}\tilde{u}_{j+\frac{1}{4}-m+j_0}^{n-\frac{1}{4}} &= \tilde{u}_{m'+\left(\frac{3}{4}-\delta j\right)}^{n-\frac{1}{2}+\frac{1}{4}} \\ &= \tilde{u}_{m'}^{n-\frac{1}{2}} + \left(\frac{3}{4} - \delta j\right)\Delta p\,(\tilde{u}_p)_{m'}^{n-\frac{1}{2}} + \frac{\Delta t}{4}(\tilde{u}_t)_{m'}^{n-\frac{1}{2}};\end{aligned} \tag{6.10}$$

if $-\frac{1}{2} \le \delta j \le \frac{1}{4}$, $\tilde{u}^{n-\frac{1}{4}}_{j+\frac{1}{4}-m+j_0}$ can be approximated as

$$\begin{aligned}\tilde{u}^{n-\frac{1}{4}}_{j+\frac{1}{4}-m+j_0} &= \tilde{u}^{n-\frac{1}{2}+\frac{1}{4}}_{m''-\left(\frac{1}{4}+\delta j\right)} \\ &= \tilde{u}^{n-\frac{1}{2}}_{m''} - \left(\frac{1}{4}+\delta j\right)\Delta p\,(\tilde{u}_p)^{n-\frac{1}{2}}_{m''} + \frac{\Delta t}{4}(\tilde{u}_t)^{n-\frac{1}{2}}_{m''}.\end{aligned} \tag{6.11}$$

in the above and hereafter $m' = j - m + j' - \frac{1}{2}$ and $m'' = j - m + j' + \frac{1}{2}$

The approximation of the integral of Eq. (6.6) within $\mathrm{CE}_-(j,n)$ is

$$\begin{aligned}\int_{\mathrm{CE}_-(j,n)} p\left(\int_{-\infty}^{\infty}\tilde{u}(q,t)\tilde{u}(p-q,t)dq\right)d\tau = p_{j-\frac{1}{4}}\frac{\Delta p}{2}\frac{\Delta t}{2} \\ \times\sum_m\left\{\left[\tilde{u}^{n-\frac{1}{2}}_m + (\tilde{u}_{\bar{p}})^{n-\frac{1}{2}}_m + \frac{\Delta t}{4}(\tilde{u}_t)^{n-\frac{1}{2}}_m\right]\tilde{u}^{n-\frac{1}{4}}_{j-\frac{1}{4}-m+j_0}\right\}.\end{aligned} \tag{6.12}$$

If $-\frac{1}{4} \le \delta j \le \frac{1}{2}$, $\tilde{u}^{n-\frac{1}{4}}_{j-\frac{1}{4}-m+j_0}$ can be approximated as

$$\begin{aligned}\tilde{u}^{n-\frac{1}{4}}_{j-\frac{1}{4}-m+j_0} &= \tilde{u}^{n-\frac{1}{2}+\frac{1}{4}}_{m'+\left(\frac{1}{4}-\delta j\right)} \\ &= \tilde{u}^{n-\frac{1}{2}}_{m'} + \left(\frac{1}{4}-\delta j\right)\Delta p\,(\tilde{u}_p)^{n-\frac{1}{2}}_{m'} + \frac{\Delta t}{4}(\tilde{u}_t)^{n-\frac{1}{2}}_{m'};\end{aligned} \tag{6.13}$$

if $-\frac{1}{2} \le \delta j \le -\frac{1}{4}$, $\tilde{u}^{n-\frac{1}{4}}_{j-\frac{1}{4}-m+j_0}$ can be approximated as

$$\begin{aligned}\tilde{u}^{n-\frac{1}{4}}_{j-\frac{1}{4}-m+j_0} &= \tilde{u}^{n-\frac{1}{2}+\frac{1}{4}}_{m''-\left(\frac{3}{4}+\delta j\right)} \\ &= \tilde{u}^{n-\frac{1}{2}}_{m''} - \left(\frac{3}{4}+\delta j\right)\Delta p\,(\tilde{u}_p)^{n-\frac{1}{2}}_{m''} + \frac{\Delta t}{4}(\tilde{u}_t)^{n-\frac{1}{2}}_{m''}.\end{aligned} \tag{6.14}$$

It must be noted that m, m', and m'' are in the computational domain we defined. For example, assuming that spatial index belongs to $[j_I, j_F]$ at $t^{n-\frac{1}{2}}$.

(a) In Eqs. (6.10) and (6.13), the index m must satisfy both of the restrictions (i) $j_I \le m \le j_F$ and (ii) $j_I \le m' \le j_F$.

While $j \ge j_I + j_F - j' + 1/2$, we consider $\tilde{u}^{n-\frac{1}{4}}_{j+\frac{1}{4}-m+j_0}$ in the interval

$$j - j_F + j' - \frac{1}{2} \le m \le j_F;$$

while $j \le j_I + j_F - j' + 1/2$, we consider the interval

$$j_I \le m \le j - j_I + j' - \frac{1}{2}.$$

(b) In Eqs. (6.11) and (6.14), the index m must satisfy both of the restrictions (i) $j_I \le m \le j_F$ and (ii) $j_I \le m'' \le j_F$.

While $j \ge j_F + j_I - j' - 1/2$, we consider $\tilde{u}^{n-\frac{1}{4}}_{j+\frac{1}{4}-m+j_0}$ in the interval

$$j - j_F + j' + \frac{1}{2} \le m \le j_F;$$

while $j \le j_F + j_I - j' - 1/2$, we consider the interval

$$j_I \le m \le j - j_I + j' + \frac{1}{2}.$$

In addition, one has

$$\int_{CE_{\pm}(j,n)} p^3\, \tilde{u}\, d\tau = \Delta p\, \Delta t \left(p_{j\pm\frac{1}{4}}\right)^3 \left[\tilde{u}_{j\pm\frac{1}{2}}^{n-\frac{1}{2}} \mp (\tilde{u}_{\bar{p}})_{j\pm\frac{1}{2}}^{n-\frac{1}{2}} + \frac{\Delta t}{4}(\tilde{u}_t)_{j\pm\frac{1}{2}}^{n-\frac{1}{2}}\right]. \tag{6.15}$$

Requiring that $\tilde{u} = \tilde{u}(p,t;j,n)$ satisfies Eq. (6.3) within SE(j,n), one has

$$\begin{aligned}(\tilde{u}_t)_{j\pm\frac{1}{2}}^{n-\frac{1}{2}} &= -\frac{1}{2\sqrt{2\pi}}\, i\, p_{j\pm\frac{1}{2}} \int_{-\infty}^{\infty} \tilde{u}\left(q, t^{n-\frac{1}{2}}\right) \tilde{u}\left(p_{j\pm\frac{1}{2}} - q, t^{n-\frac{1}{2}}\right) dq + i\, p_{j\pm\frac{1}{2}}^3 \tilde{u}_{j\pm\frac{1}{2}}^{n-\frac{1}{2}} \\ &= -\frac{1}{2\sqrt{2\pi}}\, i\, p_{j\pm\frac{1}{2}} \sum_m \left(\tilde{u}_m^{n-\frac{1}{2}}\, \tilde{u}_{j\pm\frac{1}{2}-m}^{n-\frac{1}{2}}\right) + i\, p_{j\pm\frac{1}{2}}^3 \tilde{u}_{j\pm\frac{1}{2}}^{n-\frac{1}{2}}.\end{aligned} \tag{6.16}$$

With the aid of Eqs. (6.6), (6.9), (6.15), and (6.16), $\tilde{u}_j^n$ and $(\tilde{u}_{\bar{p}})_j^n$ can be solved in terms of $\tilde{u}_{j\pm\frac{1}{2}}^{n-\frac{1}{2}}$ and $(\tilde{u}_{\bar{p}})_{j\pm\frac{1}{2}}^{n-\frac{1}{2}}$. This constitutes the time-marching scheme.

6.2 Numerical Results

Consider Eq. (6.3)

$$\tilde{u}_t + \frac{1}{2\sqrt{2\pi}}\, i\, p \int_{-\infty}^{\infty} \tilde{u}(q,t)\, \tilde{u}(p-q,t)\, dq - i\, p^3\, \tilde{u} = 0. \tag{6.3}$$

It has an exact solution

$$\tilde{u}_e(p,t) = 6p\sqrt{\pi}\, \mathrm{csch}\frac{\pi p}{\sqrt{c}} \exp(-i\, p\, c\, t). \tag{6.17}$$

It is the solitary wave solution that has behavior similar to the superposition principle. Despite the fact that the wave itself was highly nonlinear, it maintains the shape while travelling mat constant speed c.

The initial values are given by Eq. (6.17) at $t = 0$. The numerical results of $c = 0.5$ at $t = 4$ are shown in Figs. 6.2 and 6.3.

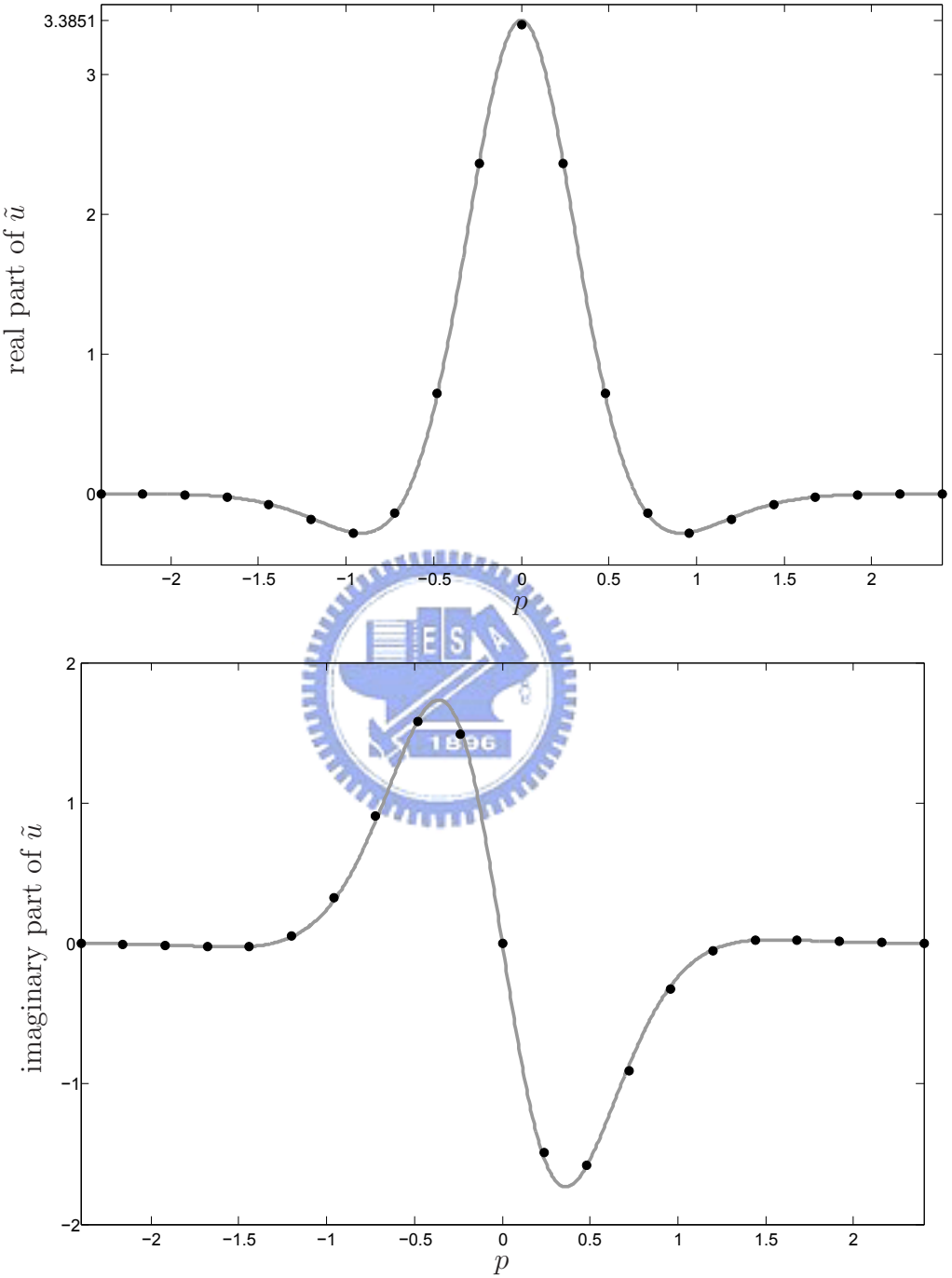

Figure 6.2. Computation result at $t = 4$ obtained with $p \in [-2.4, 2.4]$, $\Delta p = 0.24$, and $\Delta t = 0.05$

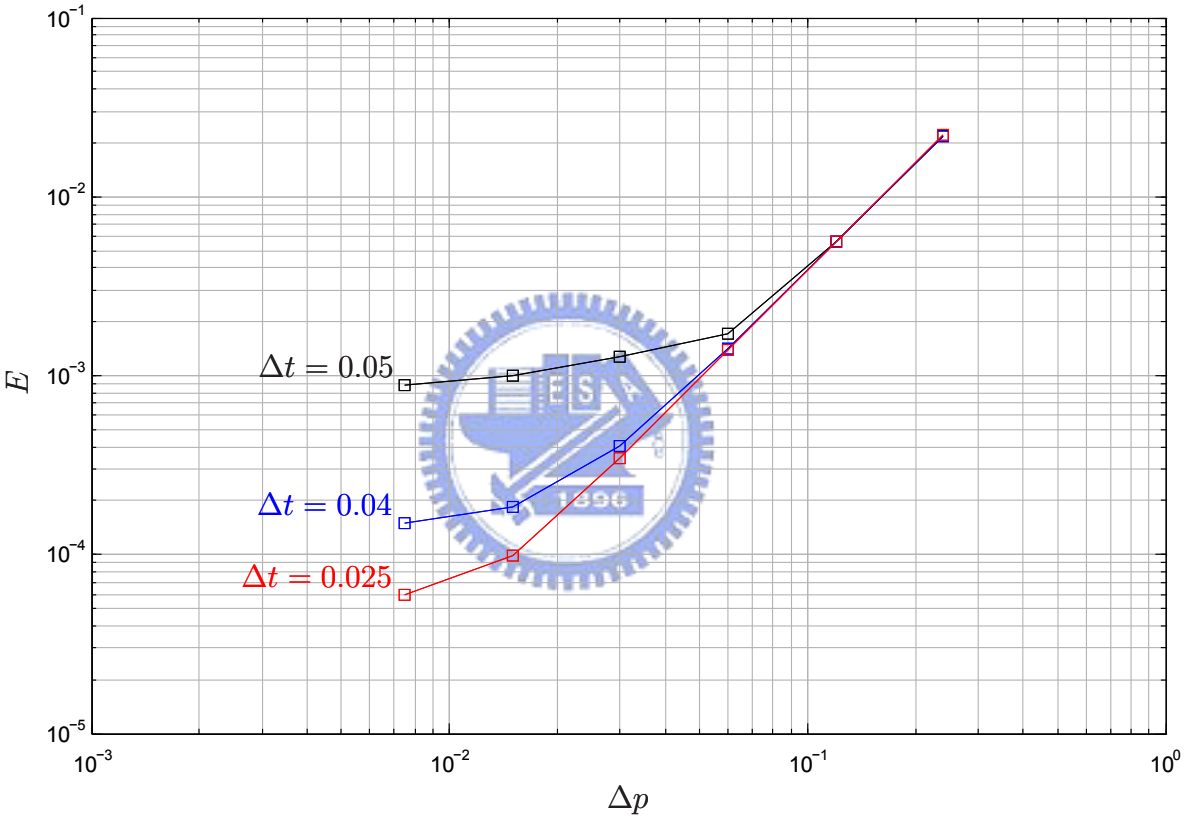

Figure 6.3. Numerical errors with $\Delta t = 0.05$, 0.04, and 0.025.

Chapter 7

Conclusions

In this thesis, we developed the CESE method in momentum space. We investigated the basic 1D wave equation, convection-diffusion equation, a driven quantum mechanical problem and the nonlinear KdV equation. The scope is on the fundamental part. We calibrate each system with known exact solution. We showed that the p-space CESE method works well for the systems from classical wave equation, nonlinear equation to quantum mechanical problem. The main advantages, in addition to the superior CESE method in coordinate space are twofold. First, the boundary conditions can be handled naturally, that is, for sufficient large momentum value, the function and its derivatives are simply vanishing. Second, the whole wave function preserved inside the p-space without flowing out from the boundary as coordinate space method. This is especially useful in treating scattering problems.

Strictly speaking, the method used in this work is not regular a-scheme. But it is still capable of generating highly accurate solution by using only the concept of flux conservation and simple approximation techniques.

In the future, we will develop the p-space CESE method to practical useful in solving realistic time-dependent problems.

References

1. S.C. Chang, W.M. To, A New Numerical Framework for Solving Conservation Laws– The Method of Space-Time Conservation Element and Solution Element, NASA TM 104495, August 1991.

2. S.C. Chang, The Method of Space-Time Conservation Element and Solution Element– A New Approach for Solving the Navier Stokes and Euler Equations, J. Comp. Phys.,vol. 119 (1995) pp. 295–324.

3. S.C. Chang, X.Y. Wang and C.Y. Chow, The Space-Time Conservation Element and Solution Element Method: A New High-Resolution and Genuinely Multidimensional Paradigm for Solving Conservation Laws, J. Comp. Phys., vol. 156 (1998) pp.89–136.

4. Z.C. Zhang, X.Y. Wang and S.C. Chang, The Space-Time CE/SE Method for the Navier-Stokes Equations in Three Spatial Dimensions, AIAA Paper 2000–2331.

5. Z.C. Zhang, S.T. Yu and S.C. Chang, Space-Time Conservation Element and Solution Element Method for Solving the Two- and Three-Dimensional Unsteady Euler Equations Using Quadrilateral and Hexahedral Meshes, J. Comp. Phys. 175, 168–199 (2002).